processes

MDPI

Review

Synthesis and Water Treatment Applications of Nanofibers by Electrospinning

Saumya Agrawal [1,†], Rashmi Ranjan [1,†], Bajrang Lal [1], Ashiqur Rahman [2,*], Swatantra P. Singh [1,3,4,*], Thinesh Selvaratnam [2,5] and Tabish Nawaz [1,*]

1 Environmental Science and Engineering Department, Indian Institute of Technology Bombay, Mumbai 400076, India; saumyaagrawal@iitb.ac.in (S.A.); 19I180001@iitb.ac.in (R.R.); bajrang_jat@iitb.ac.in (B.L.)
2 Center for Midstream Management and Science, Lamar University, Beaumont, TX 77705, USA; tselvaratnam@lamar.edu
3 Centre for Research in Nanotechnology & Science (CRNTS), Indian Institute of Technology Bombay, Mumbai 400076, India
4 Interdisciplinary Program in Climate Studies, Indian Institute of Technology Bombay, Mumbai 400076, India
5 Department of Civil & Environmental Engineering, Lamar University, Beaumont, TX 77710, USA
* Correspondence: arahman2@lamar.edu (A.R.); swatantra@iitb.ac.in (S.P.S.); tnawaz@iitb.ac.in (T.N.)
† Both authors have contributed equally to the work.

Abstract: In the past few decades, the role of nanotechnology has expanded into environmental remediation applications. In this regard, nanofibers have been reported for various applications in water treatment and air filtration. Nanofibers are fibers of polymeric origin with diameters in the nanometer to submicron range. Electrospinning has been the most widely used method to synthesize nanofibers with tunable properties such as high specific surface area, uniform pore size, and controlled hydrophobicity. These properties of nanofibers make them highly sought after as adsorbents, photocatalysts, electrode materials, and membranes. In this review article, a basic description of the electrospinning process is presented. Subsequently, the role of different operating parameters in the electrospinning process and precursor polymeric solution is reviewed with respect to their influence on nanofiber properties. Three key areas of nanofiber application for water treatment (desalination, heavy-metal removal, and contaminant of emerging concern (CEC) remediation) are explored. The latest research in these areas is critically reviewed. Nanofibers have shown promising results in the case of membrane distillation, reverse osmosis, and forward osmosis applications. For heavy-metal removal, nanofibers have been able to remove trace heavy metals due to the convenient incorporation of specific functional groups that show a high affinity for the target heavy metals. In the case of CECs, nanofibers have been utilized not only as adsorbents but also as materials to localize and immobilize the trace contaminants, making further degradation by photocatalytic and electrochemical processes more efficient. The key issues with nanofiber application in water treatment include the lack of studies that explore the role of the background water matrix in impacting the contaminant removal performance, regeneration, and recyclability of nanofibers. Furthermore, the end-of-life disposal of nanofibers needs to be explored. The availability of more such studies will facilitate the adoption of nanofibers for water treatment applications.

Keywords: nanofiber; electrospinning; heavy-metal remediation; desalination; contaminants of emerging concern remediation

Citation: Agrawal, S.; Ranjan, R.; Lal, B.; Rahman, A.; Singh, S.P.; Selvaratnam, T.; Nawaz, T. Synthesis and Water Treatment Applications of Nanofibers by Electrospinning. *Processes* **2021**, *9*, 1779. https://doi.org/10.3390/pr9101779

Academic Editor: Farooq Sher

Received: 22 July 2021
Accepted: 23 September 2021
Published: 6 October 2021

1. Introduction

Nanotechnology is revolutionizing the world through its incredible potential in a wide range of applications such as electronics, power sources, medical treatments, industrial applications, defense systems, construction materials, and environmental remediation, such as water treatment and air purification. One such example of nanotechnology is

nanofibers. Nanofibers are polymeric fibers having a diameter in the nanometer to submicron range. They can be synthesized from different polymeric precursors with suitable solvents. Natural and synthetic polymers are used to prepare polymeric solutions, which are further processed for nanofiber synthesis [1–4]. Nanofibers possess extremely high specific surface area, low density, high porosity, and the ability to form a highly porous matrix with excellent interconnectivity between their pores. Nanofibers are also quite amenable to tunability in terms of their properties and can be tailormade according to the process requirements by controlling the synthesis parameters. Additionally, a large specific area of the nanofibers allows incorporating specific functionality by immobilizing nanoparticles, zeolites, metal–organic frameworks, etc. This leads to the enhancement of the selectivity, kinetics, and capacity of the contaminant removal processes. Nanofiber-based applications are convenient from the mode of contacting perspective as they can be packed in a fixed-bed column or utilized as a membrane reactor depending on the separation process requirements. These properties make nanofibers suitable for applications in almost every aspect of human life. They have potential applications in drug delivery, biomedical industry, energy storage, protective clothing, and environmental remediation. Nanofibers serve as a promising platform for numerous environmental applications, especially in water treatment for removing specific contaminants such as heavy metals, persistent organic pollutants (POPs), contaminants of emerging concern (CECs), and oily molecules, as well as desalination and particulate matter and organic pollutant removal for air filtration devices [5].

Both natural and synthetic polymers are used for nanofiber synthesis [6]. Synthetic polymers are widely used owing to their low cost, ease of production, and high mechanical properties. However, most petroleum-based synthetic polymers can cause severe long-term health and environmental concerns in disposal because of their nonbiodegradable and toxic nature. The nanofibers synthesized using petroleum-derived synthetic polymers will persist in the environment for a long time. Therefore, there is a need to minimize waste generation by maximum utilization of materials in the process or using recyclable and biodegradable materials [7]. Industrial and academic researchers have now started focusing on green polymers for nanofiber synthesis instead of synthetic polymers derived from petroleum because of their sustainable and environmentally friendly nature [8].

Various techniques of polymeric nanofiber synthesis have been reported in the literature. Electrospinning is considered one of the most widely used nanofiber synthesis methods along with several non-electrospinning techniques such as phase separation, self-assembly, and interfacial polymerization of nanofibers. Electrospinning is a simple, controlled, and effective technique for synthesizing polymeric nanoscale to submicron-sized fibers. In general, electrospun nanofibers provide desirable performance due to their unique nanostructures with substantially high surface area, small interstitial spaces, porous structures, and high interconnectivity between the fibers. The electrospinning process parameters can be tuned to fabricate nanofibers of desired properties such as thickness, porosity, hydrophilicity, and polarity. The variation in electrospinning operating parameters and precursor raw material composition (precursor polymer, solvent, and other application-specific additives) imparts diverse tunable properties to nanofibers and make them versatile for various applications.

This review article presents the fundamentals of the electrospinning technique and the impact of the synthesis process parameters on nanofiber properties. Subsequently, the application of nanofibers for various water treatment applications such as desalination, heavy-metal remediation, and removal of CECs is discussed. The literature survey was conducted for the abovementioned specific applications to present the latest state-of-the-art nanofiber technologies. Furthermore, their advantages and limitations are discussed.

2. Nanofiber Synthesis: Electrospinning Process

Electrospinning is the process of fabrication of nano to micron diameter fibers via the application of high voltage to the polymer solution [9]. These fibers have a larger

specific surface area than fibers obtained via the conventional spinning process [10]. Both electrospinning and electrospraying are considered sister electrohydrodynamic methods, working on the same principle. The major difference between electrospraying and electrospinning is the stability of the electrified polymer jet, controlled by two types of instability, i.e., Rayleigh instability and whipping instability. Rayleigh instability occurs due to the solution's surface tension, which reduces the surface area by forming droplets, i.e., electrospraying. By increasing the applied voltage, Rayleigh instability is suppressed. The presence of electrostatic forces produces whipping instability that causes bending and stretching of the jet essential for forming thin fibers, i.e., electospinning. The different forces acting on a liquid droplet are shown in Figure 1. These forces cause the Rayleigh instability and whipping instability leading to the formation of nanofibers. These electrohydrodynamic techniques consist of a syringe filled with polymeric solution fitted with a metal needle for electrospraying, which is connected with a high-voltage power source and collector at the bottom [9,10]. It can utilize various materials such as synthetic and natural polymer solutions, emulsions, suspensions, ceramics, metals, and composite systems. Electrospinning has the advantage of being a simple, fast, versatile, and cost-effective technology with limitations such as low productivity and small pore size [10].

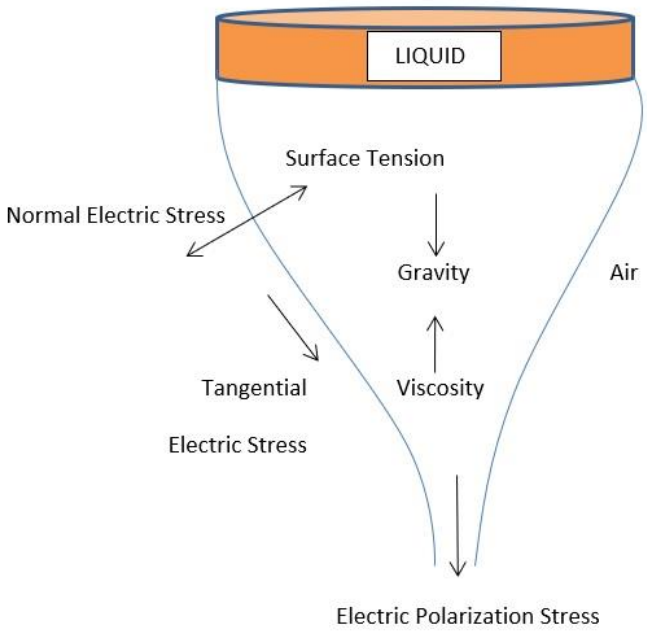

Figure 1. Diagrammatic description of forces active in nanofiber formation during electrospinning [11].

A jet from an electrified liquid droplet is generated during electrospinning, which subsequently stretches and elongates to fabricate nanofibers due to the forces acting on the droplet (Figure 1). The induction of charges within the fluid reaches a critical high-voltage level (5–25 kV), leading to the eruption of a fluid jet at the tip of the needle from the polymer solution droplet, which takes the shape of a cone referred to as Taylor's cone. The flowing jet travels toward the lower-potential region, i.e., the collector region, and away from the needle tip. The solvent gets rapidly vaporized during the flight time from the fluid jet, and the entanglements of these polymer chains prevent them from breaking. As a result, these polymer chains are collected on the collector in the form of nanofibers. The jet surface discharges as it reaches the collector, and solid products (ultrafine polymer fibers) are formed on the metallic collector [9,10].

In general, the formation of electrospun fibers can be divided into four regions as shown in Figure 2: (1) charging of liquid droplets at the needle tip and formation of Taylor cone (Taylor cone region); (2) extension of the jet in the form of a straight line (straight jet); (3) thinning of polymer jet under the influence of electrostatic force and growth of

electrical bending instability, i.e., whipping instability (whipping jet); (4) dry deposition and solidification of fiber on collecting surface.

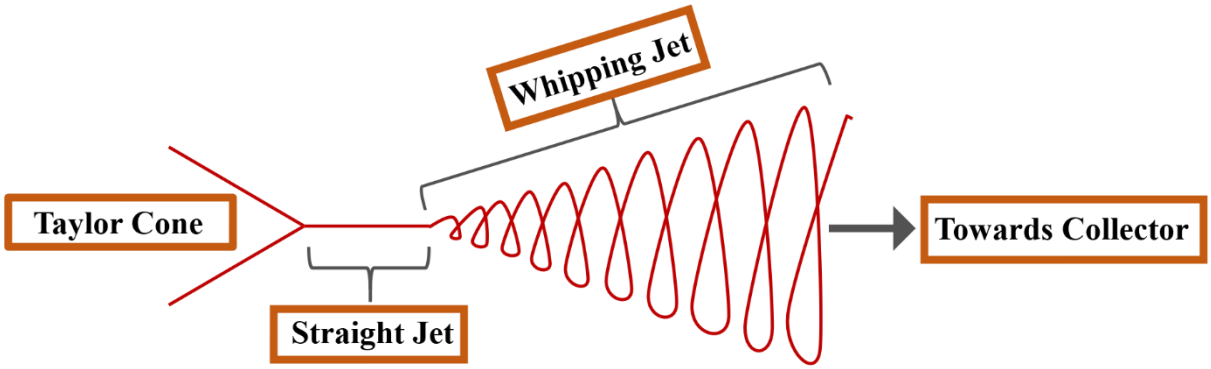

Figure 2. The different stages of electrospun jet leading to nanofiber formation [12].

The setup of the electrospinning system consists of three major components in a closed chamber: a high-voltage power supply, a spinneret (a syringe with a pump through which the polymer solution is fed through a capillary connected to a syringe filled with polymeric solution), and a grounded collecting plate (usually a metal screen, plate, or rotating mandrel). As shown in Figure 3, the electrospinning setup can be vertically oriented or horizontally oriented [10]. Rodoplu and Mutlu (2012) [13] observed that, in the horizontal electrospinning setup, the polymer droplets showed a tendency to exhibit a projectile motion with the increasing voltage, while fibers were collected downward of the collector plate; on the other hand, in the vertical electrospinning setup, it was reported that the location for collection of polymer fiber on the collector was random and not on the center of the collector plate due to the condition of bending instability (whipping instability).

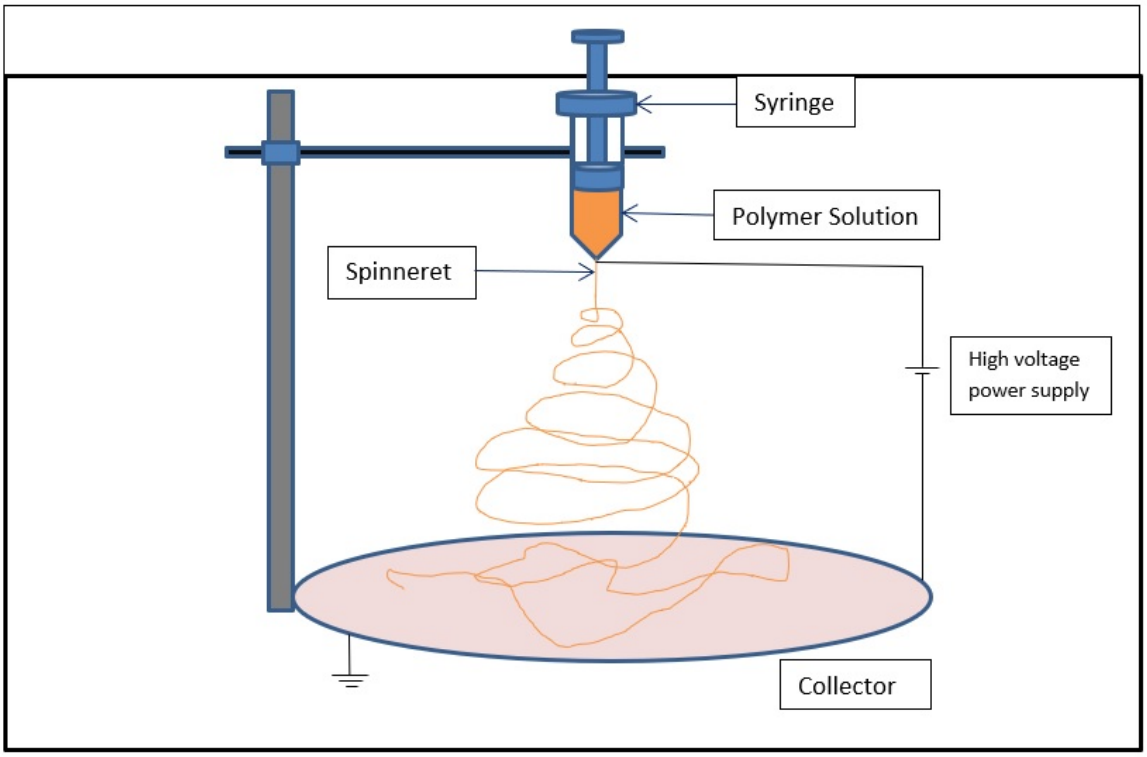

Figure 3. *Cont.*

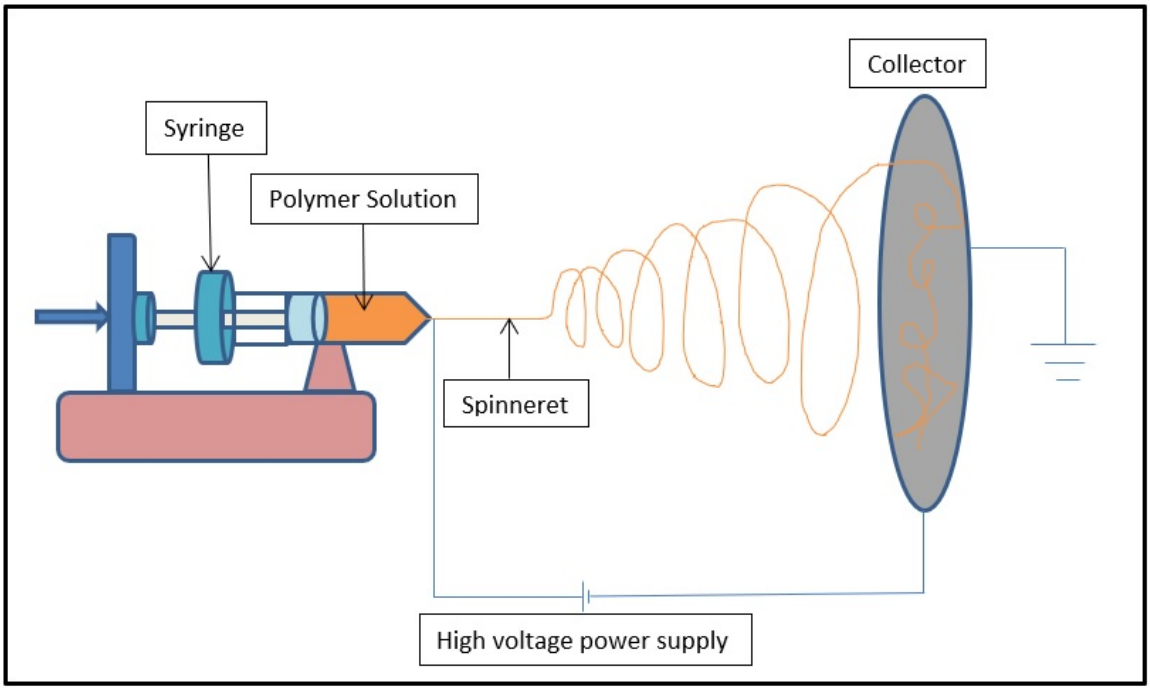

Figure 3. The vertical and horizontal orientations of the electrospinning setup [10].

2.1. Effect of Electrospinning Parameters on Nanofiber Properties

The nanofiber morphology and size are greatly determined by the feed polymeric solution parameters (concentration, molecular weight, solvent, viscosity, conductivity, surface tension, and the addition of polyelectrolyte) and electrospinning process parameters (applied voltage, tip to collector distance, and flow rate) [14]. Different nanofibers with different morphologies, structures, and arrangements can be created by understanding these parameters and varying them.

2.1.1. Solution Parameters

Polymer Concentration

Polymeric solution concentration is one of the deciding factors of fiber morphology in the electrospinning process. For the preparation of a continuous fiber through electrospinning, an optimum polymer solution concentration is required, which can overcome the surface tension with polymer chain entanglement. However, beads are formed at low concentrations instead of fibers as electrospraying dominates electrospinning; thus, surface tension force overcomes the electrostatic and viscoelastic force, leading to the dominance of Rayleigh instability. In contrast, at too high concentrations, fabrication of continuous fibers is prohibited due to high viscoelasticity and difficulty in maintaining the flow at the tip of the needle, causing the formation of large-diameter fibers or discontinuous fibers [15]. With the increase in solution concentration, it was found that the beads changed their shape from spherical to spindle-like, and uniform fibers with increased diameters were finally formed due to viscosity resistance [16–18]. Williams et al. (2019) [19] established a power-law relationship between the solution concentration and fiber diameter for electrospinning gelatin-like polymers, which emphasized that, by increasing the concentration of a solution, the fiber diameter is increased.

Molecular Weight of the Polymer and Solution Viscosity

The molecular weight (MW) of the polymer and the viscosity of the solution are interconnected. Solution viscosity represents the degree of entanglement of the polymer solution. It has been observed that the entanglement and the overlapping of low-molecular-weight polymeric chains are not efficient. They easily flow past each other, forming a

low-viscosity solution that favors Rayleigh instability, and beaded fibers are obtained. Nevertheless, high-molecular-weight polymers show effective overlapping and entanglement, overcoming Rayleigh instability and forming enlarged nanofiber chains. The viscosity of the solution is highly affected by polymer MW, its concentration, and solvent characteristics. Therefore, viscosity can be varied by changing the solvent and/or polymer concentration. It is necessary to have an optimum viscosity with a higher or optimum solution concentration to enable electrospinning. On the other hand, if the solution viscosity is too high, it will be difficult for the polymer jet to elongate, and narrower and thicker fibers are formed [20,21]. Furthermore, too high a viscosity will also make it very difficult to pump the solution through the syringe needle for electrospinning [22], and the solution may dry at the tip of the needle before the electrospinning starts [23,24]. The range of viscosity at which spinning is done varies with the different polymer solutions. A literature review reported a maximum spinning viscosity range from 1 to 215 poise [20,25,26].

Surface Tension of the Solution

To gear up the electrospinning process, electrostatic forces must overcome the forces due to surface tension. Surface tension may cause the formation of beads along with the jet as it travels toward the collector. It tends to decrease the surface area per unit mass of the fluid. Therefore, at a high concentration of free solvent molecules, the solvent molecules can congregate and form a spherical shape due to surface tension. At higher viscosity, there is prominent interaction between the solvent and polymer molecules. Therefore, when the solution is stretched under the influence of charges, the solvent molecules will tend to spread over the entangled polymer molecules, thereby reducing the effect of surface tension [9]. Different solvents may contribute to different surface tension. With the addition of an insoluble surfactant which is dispersed in a solution as a fine powder, the fiber morphology is also improved [27].

Conductivity of the Solution

The conductivity of a polymeric solution influences the stretching of the polymeric droplet at the needle's tip caused by the repulsion of the charges at the droplet's surface. The solution conductivity is mainly affected by the type of the polymer, the nature of the solvent used, and the presence of ions. Juliana et al. (2018) [28] fabricated polyimide fibers with four different solvents, NMP, DMSO, DMF, and DMAC, and it was observed that DMSO had a higher electrical conductivity than NMP, with the type of solvent affecting the conductivity of the polymer solution. In addition, DMSO solutions showed sudden transitions from beads to fiber, whereas NMP solutions had a smooth transition to homogeneous fibers. With higher conductivity, smooth fibers are formed instead of beaded fibers. However, the increased stretching of the solution will tend to form nanofibers with smaller diameters [23]. The critical voltage for electrospinning is also reduced in the presence of ions, which increases the conductivity [29]. Higher conductivity causes greater bending instability, resulting in an increase in the deposition area of the fiber [30], which favors the formation of finer fibers since the jet path is now increased.

Solvent Type

The solvent used for making the polymeric solution is critical in synthesizing uniform, porous, defect-free, and beadless electrospun nanofibers. The critical minimum concentration Ce (minimum concentration needed for forming beaded nanofibers) of the polymeric solution, depends on the molecular chain length, chemical properties of the polymer, and the solvent selected. The choice of solvent for making a polymeric solution becomes very important when a particular polymer of a specific molecular weight and molecular chain length is used to make electrospun nanofibers. The nanofiber morphology is determined by the solvent characteristics such as boiling point, dielectric constant, surface tension, concentration, conductivity, and viscosity [31]. The solvents having high conductivity and high dielectric constant create high charge density on the droplet's surface at the needle tip.

These charges carried by the jet lead to self-repulsion under the electric field, producing small-diameter fibers and a straight shape. An increase in solvent viscosity prevents stretching of the jet segment, forming fibers of large diameter. Solvents having a low dielectric constant, dipole moment, and high volatility result in poor nanofiber productivity. Highly volatile solvents such as alcohol form nanofibers with increased diameters, resulting from the weak elongation forces acting on the jet. The solvent–polymer interaction affects the overall properties of the polymeric solution, and a proper solvent selection can be made using simulation studies. Lu et al. (2006) [31], using computer simulation, indicated that the molecular energy and the orientation barrier of the molecule chain vary with the kind of solvents used in making the polymeric solution. They also determined that, in the case of water as a solvent, the molecule is rigid with lower energy because of the presence of strong interactions such as hydrogen bonds between monomer units and water molecules. The formation of hydrogen bonds by the solvent molecule with the polymer molecule decreases the molecule energy, leading to a stable configuration and molecular rigidity. The molecular flexibility indicates the orientation ability of the molecule. The molecule's orientation is easy if it is flexible and, hence, jet instability is prominent, leading to the formation of nanofibers with a small diameter. Due to the solvent–polymer molecular interaction via hydrogen bonding, rearrangement energy is needed during the orientation of the molecule chain to overcome the hydrogen bonding [32]. There should be sufficient molecular energy to provide enough flexibility for molecular chains to orient in smooth and straight nanofibers of small diameters. Therefore, it is crucial to properly select a solvent on the basis of its chemical properties and the interaction with the polymeric species. In low-concentration polymer solution, increased volatilization of the solvent occurs due to high solvent content, leading to fibers having micro-holes. With the regulation of the intrinsic properties of the polymer solution, fiber morphology can be controlled, and web density and porosity can be determined from the way in which fibers assemble [32]. The difference in solubility of each component in the system may affect the fiber diameter and diameter distribution [33]. Luo et al. (2010) [34] suggested that lower solubility favors the formation of good electrospinnable polymeric solutions. Spinnability–solubility maps were developed to simplify the solvent selection procedure by accepting mixed solvent systems to be formed using a geometrical method based on the solubility region of the polymer. Porous fibers were synthesized from a solution of the binary solvent system formed by mixing a highly soluble solvent and a nonsolvent such as dimethyl sulfoxide (DMSO) in which both solvents have low volatility [34]. Evaporation of solvent plays a crucial role in the synthesis process. Rapid solvent evaporation along with the jet stretching by electric forces and jet destabilization is eventually responsible for the shape, size, structure, and properties of synthesized nanofibers [35].

2.1.2. Electrospinning Process Parameters

Voltage

The application of high voltage plays a crucial role in the electrospinning process. A high-voltage power induces a spherical droplet to become unstable, acquiring a conical shape and forming ultrathin nanofibers at critical voltage. The applied critical voltage differs from one polymeric solution to another, and there is an optimum range of the electric field strength for a particular polymer–solvent system which results in smooth nanofibers of small diameter. Any increase or decrease in the applied voltage beyond this critical voltage will result in nanofibers with beads. A voltage of magnitude greater than 6 kV can form Taylor's cone during jet initiation in the electrospinning of a PEO (polyethylene oxide)/water system, forming bead-free nanofibers. A critical voltage range of 5.5–9 kV was determined for the electrospinning of the PEO/water system. An increase in the applied voltage in the given range showed an increase in bead formation due to increased current flow through the polymeric solution. Beyond 7 kV, beads on the nanofibers were prevalent and highly dense due to increased voltage. As the applied voltage and resultant electric field can both influence the stretching and acceleration of the jet, they can affect the

morphology of fiber formation. A voltage close to the critical voltage for electrospinning may be favorable to form finer fibers [36]. Zhong et al. (2002) [23] reported that the shape of the bead varies from spindle-like to spherical-like with an increase in voltage. A higher voltage causes more polymer ejection; thus, the formation of larger-diameter fibers takes place [24,37].

Solution Flow Rate

The flow rate of the polymeric solution through the syringe pump influences the ensuing jet velocity and rate of polymer transfer, thereby affecting the morphology of the nanofibers. To maintain the shape of the Taylor cone at the syringe orifice and synthesize bead-free nanofibers, a minimum flow rate of the polymer solution is crucial [38]. With increased flow rate, the available polymer volume increases, resulting in nanofibers of increased diameter and pore size. High flow rate also leads to ineffective drying of the nanofiber before reaching the collector, resulting in bead defects and a flattened ribbon-like structure. A lower flow rate is preferable for forming bead-free and ultrafine nanofibers, providing enough time for the solvent to evaporate [38]. A correlation between high flow rate and surface charge density was observed in the case of PEO. An increase in the flow rate of the solution simultaneously increased the electric current, thereby reducing the surface charge density on the polymeric solution droplet, resulting in the merged nanofibers [38,39].

Collector Characteristics

In electrospinning, a collector serves as a surface for nanofiber collection and, thus, has a substantial effect on the final structure and arrangement of the nanofibers. The collector conducts the charges on the deposited fibers to the ground and, thus, affects the number of fibers being collected on the substrate. The charges may be retained on the deposited fibers in the case of less conductive collectors causing repulsion to the incoming fiber, thereby decreasing the deposition of the fiber and, hence, productivity. This also poses a restriction to the achievable thickness of the nonwoven mat. Even a small change in the electric field strength on the surface of the collector can affect the deposition of the fiber. Despite the effects of the collector material on charge retention, there is a negligible effect on the thickness of the fiber. It was also observed that the type of grounding material has more influence than the supporting material on the amount of fiber collection. Fiber deposition can be facilitated on a nonconducting surface by reducing the charge density of the jet in electrospinning by the use of blower, focusing, or steering electrodes [40]. Heterogeneous substrates (having both metal and insulator) are used as a collector, which induces a distorted electric field, causing preferential deposition of fibers on the metal surface and fiber extension on the insulator region. Such substrates allow the production of patterned mats. The nanofibers can be directed to mimic the patterns of the insulating material by using the insulator to mask the grounded conductive substrate [25,26]. The generated nanofibers are deposited on the collector as a random mass due to the bending instability of the highly charged jet [41]. A simple collector plate would allow the formation of an unwoven nanofiber mat in random orientation, whereas aligned nanofibers can be collected by designing specialized collectors. A rotating drum, rotating wheel-like bobbin, or metal frame as the collector can be used for getting aligned electrospun fibers that are more or less parallel to each other [25,26].

The fiber alignment is determined by the type of the target/collector and its rotation speed [40]. The rotation speed should not be too fast as it can stretch or break fibers into small fragments. Fibers will be collected as mats if the rotation of the collector is very slow. Tip-to-collector distance is another potential parameter to control fiber size and morphology. A required minimum distance should be established to get sufficient time for the fiber to dry before reaching the collector. Bead formation takes place on either side if the distance is too close or too far [42]. A proper distance between the needle and the collector should be maintained to get optimum size nanofibers. Elongation of the jet

and thinning happen only while the jet is in flight and not yet solid; hence, increasing the distance between the collector and nozzle will increase the time for thinning to occur, producing nanofibers of small diameters [42].

2.1.3. Ambient Conditions

Ambient parameters such as temperature and humidity also have some effect on the electrospinning process. Mit-uppatham et al. (2004) [43] found that an increase in temperature results in decreased fiber diameter as the viscosity of solution decreases with increasing temperature. The effect of relative humidity depends on the interaction between the polymeric solution and the water vapor in the surrounding. Higher humidity was found to result in the formation of larger-diameter nanofiber in the case of polystyrene and polyetherimide fibers. This may be due to rapid precipitation of the polymer when water condenses on the surface of the jet, leading to a reduction in jet elongation. Beaded fibers are also formed at high humidity in the case of PVP and PEO nanofibers. The variation of humidity with polystyrene solution showed that the occurrence of small circular pores on the surface of the fibers as an increase in ambient humidity leads to coalescing of the pores [44].

With the progress of time, various developments have been achieved in the conventional electrospinning process to obtain better results and overcome the limitations. These include multi-jet electrospinning, coaxial electrospinning, emulsion electrospinning, solvent-free electrospinning, force spinning, and electrospinning by porous hollow tube. Table 1 summarizes the impact of the variation of electrospinning process parameters on the diameter, specific surface area, and mechanical strength of the nanofiber.

Table 1. Impact of electrospinning parameters on the properties of synthesized nanofibers.

Electrospinning Parameter	Nanofiber Diameter	Specific Surfaces Area of Nanofibers	Mechanical Properties of Nanofibers
Solution concentration	Direct	Inverse	Direct
Molecular weight	Direct		Direct
Viscosity	Direct		Direct
Surface tension	Inverse		Direct
Conductivity	Direct		Direct
Flow rate	Inverse	Direct	Inverse
Applied voltage	Direct		Direct
Tip to collector distance	Inverse		Inverse
Collector type	No Impact	Direct	No Impact
Temperature and humidity	Inverse		Direct with humidity and inverse with temperature

3. Applications of Nanofibers for Water Treatment

Nanofibers, due to their high specific surface area and ability to incorporate various functional groups, molecules, nanoparticles, etc. in their polymeric matrix, offer various applications in environmental remediation, including air and water treatment. Nanofibers have been used as adsorbents, photocatalytic materials, electrochemical electrodes, and membranes for a diverse range of applications from heavy-metal, organic, and CEC remediation to desalination (Figure 4). This section discusses major water treatment applications such as desalination, heavy-metal removal, and CEC removal.

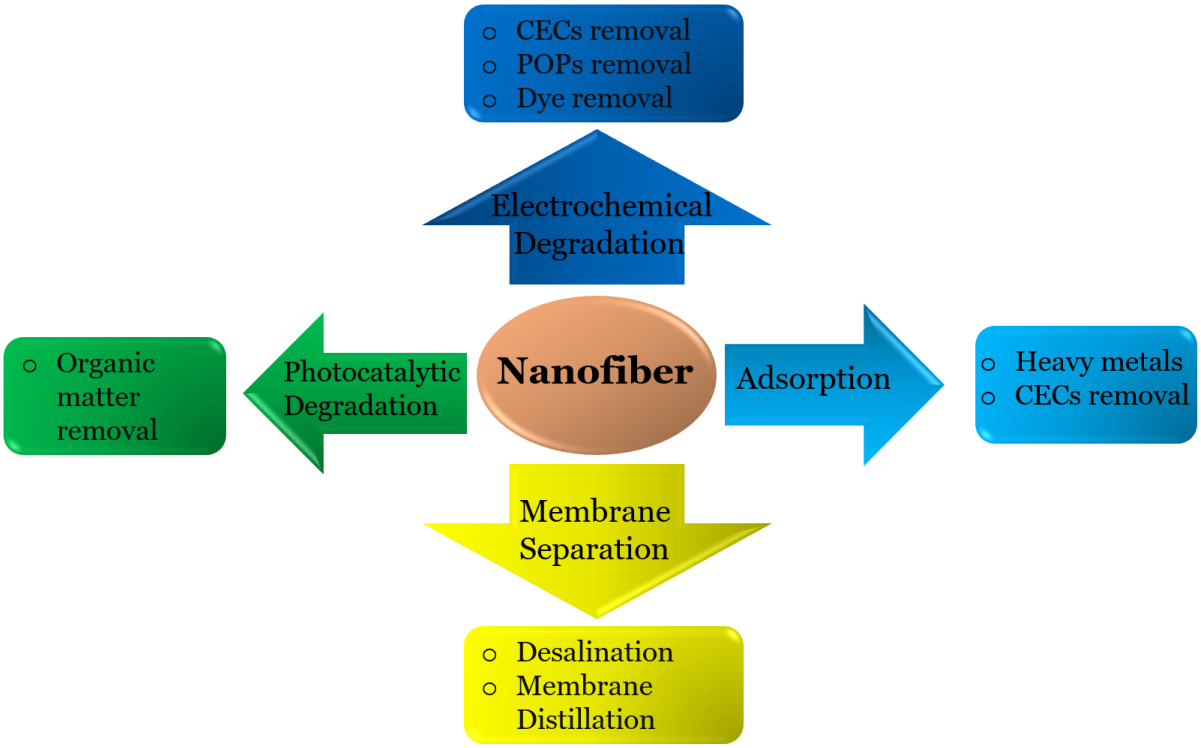

Figure 4. Water treatment applications of nanofibers.

3.1. Desalination

Nanotechnology, particularly nanofiber membranes (NFMs), is a relatively new approach for fabricating membranes for water treatment or desalination. Desalination can be achieved by thermal-based and membrane-based technologies, wherein membrane-based technologies have gained a lot of interest. Membrane-based technologies such as membrane distillation (MD), forward osmosis (FO), reverse osmosis (RO), and nanofiltration (NF) are commonly used for water desalination at different stages [45,46]. MD and RO have been extensively utilized for water desalination because of their high salt rejection efficiency (>98%) and capacity to generate potable water [46,47]. The efficiency of these technologies depends on membrane characteristics. The membrane distillation (MD) method using nanofibrous membranes is the most widely applied method for water desalination. The MD process depends on the temperature difference of the feed and permeates solution. Thus, the water vapor pressure is the driving force [48,49] across the hydrophobic membrane. The heat and mass transfer processes in MD affect the membrane hydrophobicity, wettability, porosity, etc. Membrane hydrophobicity and low porosity reduce the water flux in the MD process. The major challenge associated with the MD membrane is pore wettability, affecting the membrane stability and hydrophobicity and, thus, affecting membrane performance [50]. The MD membranes should have high permeability, high hydrophobicity, low pore wettability, and high salt rejection. MD can be used in four different configurations: direct contact membrane distillation (DCMD), air gap membrane distillation (AGMD), sweep gas membrane distillation (SGMD), and vacuum membrane distillation (VMD) [51]. Polyvinylidene fluoride (PVDF) is the most commonly utilized membrane for membrane distillation due to its high hydrophobicity, low surface energy, high thermal stability, and mechanical strength. Many different types of PVDF-based electrospun nanofiber membranes were prepared by electrospinning that gave a permeate flux of 48.8 LMH and showed good resistance to membrane scaling and wetting in DCMD configuration [52]. Improved membrane hydrophobicity and flux were observed in the case of carbon nanotube electrospun membrane used in DCMD [53].

Composite membranes based on PVDF–hexafluoropropylene (PVDF–HFP) modified by incorporating boron nitride nanosheets, graphene, carbon nanotubes, and other nanoparticles showed increased membrane hydrophobicity and liquid entry pressure (LEP), thereby decreasing the membrane wettability while maintaining the pore size large enough to get high porosity, high flux, and salt rejection (>99%) [54–57]. Omniphobic membranes were developed to decrease the wettability of the membrane caused due to feed solution composition, as these membranes are both hydrophobic and oleophobic, which resist low-surface tension liquids [58,59]. There is a tradeoff between anti-wettability and water flux in MD. To overcome this tradeoff, an approach of using a composite membrane having both hydrophobic and hydrophilic polymers was suggested [60]. Another approach to increase the membrane anti-wettability is the fabrication of a superhydrophobic nanofiber membrane which can be achieved by surface fluorination [61], PTFE incorporation [62], CNT coating [63], polydimethylsiloxane incorporation [64], and graphene oxide (GO) incorporation [65]. Superhydrophobic membranes have multilevel surface roughness and a small liquid–solid contact area, which provides the benefits of lower membrane fouling [51].

Nanofiber membranes for reverse osmosis desalination of water have also been synthesized using different polymers that showed very high salt rejection. The main challenge associated with reverse osmosis desalination is membrane fouling as RO operates at high external pressure. Higher water flux and salt rejection were observed in thin-film composite RO membranes synthesized using polyacrylonitrile (PAN) [66] and cellulose nanofibers [67,68]. A crosshatched nanofiber membrane modified by dopamine [69] showed high water flux and salt rejection (>95%), which was still lower than MD membranes that showed rejection of more than 99%. Nevertheless, these membranes show better anti-fouling behavior than many other RO membranes. The water flux in the case of FO membranes was higher compared to the MD membranes. The FO process for desalination of water has been greatly explored in recent years because of its low energy requirement, high flux, low membrane fouling, and high salt rejection properties. However, FO suffers from the reverse solute flux of the draw solution. A cellulose acetate/PVDF nanofiber support membrane designed by coaxial electrospinning reported a very low specific reverse solute flux (SRSF) of 0.03 g/L and a very high flux of 31.2 LMH [70]. These membranes having low RSF can help overcome the drawbacks of FO, where RSF leads to loss of draw solution. PAN-based thin-film composite (TFC) nanofiber FO membranes were synthesized to make hydrophilic membranes [71], which showed improved flux and salt rejection compared to the commercial cellulose triacetate (CTA) FO membrane. The effects of blending of inorganic materials with PVDF were investigated by incorporating metal oxides such as TiO_2, SiO_2, Al_2O_3, and ZrO_2. Metal oxides such as amorphous SiO_2 nanoparticles incorporated into a poly(vinylidene fluoride) (PVDF) electrospun nanofiber membrane (ENM) membrane showed a flux of 83 LMH and a salt rejection of more than 99% [72]. The performance of the membrane depends on the amount of nanoparticles being incorporated, and optimization is, therefore, required. The metal-oxide-incorporated ENM showed improved separation performance and increased the membrane anti-fouling properties, wettability, mechanical properties, and hydrophilicity [73]. This was mainly due to the change in the structure of pores caused by inorganic particle incorporation [72]. A nanofiltration membrane composed of polyamide/Kevlar aramid nanofiber prepared by nonsolvent-induced phase separation followed by interfacial polymerization remained stable for a long duration and had excellent divalent salt rejection [74]. Capacitive deionization (CDI)-based water desalination investigated using an Mn_2O_3 nanoflower-decorated electrospun carbon nanofiber membrane had high desalination capacity and also recyclability [75,76]. Many different MD, RO, FO, CDI, and NF nanofiber membranes for desalination are summarized in Table 2 with their separation properties and fabrication methods.

Nanofibers have enormous application in the desalination by FO, RO, MD, NF, and CDI [77]. Figure 5 summarizes the advantages, disadvantages and application of nanofibers in desalination using different techniques. The electrospinning process for the fabrication of nanofibrous membranes provides a high surface-area-to-volume ratio, homogeneous pore distribution, and enhanced pore interconnectivity in the membranes [78]. An electrospun nanofiber membrane can be easily modified by surface treatments, plasma treatment, surface grafting, nanoparticle incorporation, layer-by-layer coating, and interfacial polymerization to form thin-film composites to enhance membrane characteristics suited for the technology being used. Nanofibrous membranes have great potential for wastewater treatment, heavy-metal removal [79], geothermal desalination [78], and ecological remediation of highly concentrated waste streams. It is important to regulate the pore size of the nanofiber membrane in agreement with the required efficiency of filtration. Although highly explored in the laboratory, these membranes have gained limited accomplishment in commercial-scale utilization [80,81]. There are only a few units that utilize nanofiber-based membranes. Most of the large-scale desalination units utilize the RO process. Nanofiber membranes having a low fouling tendency, high salt rejection, high water flux, and low reverse salt flux can be used in integrated FO–MD or FO–RO systems in the future to obtain pure water for drinking purposes. The integrated systems utilizing nanofiber membranes can be promising for industrial applicability to reclaim potable water.

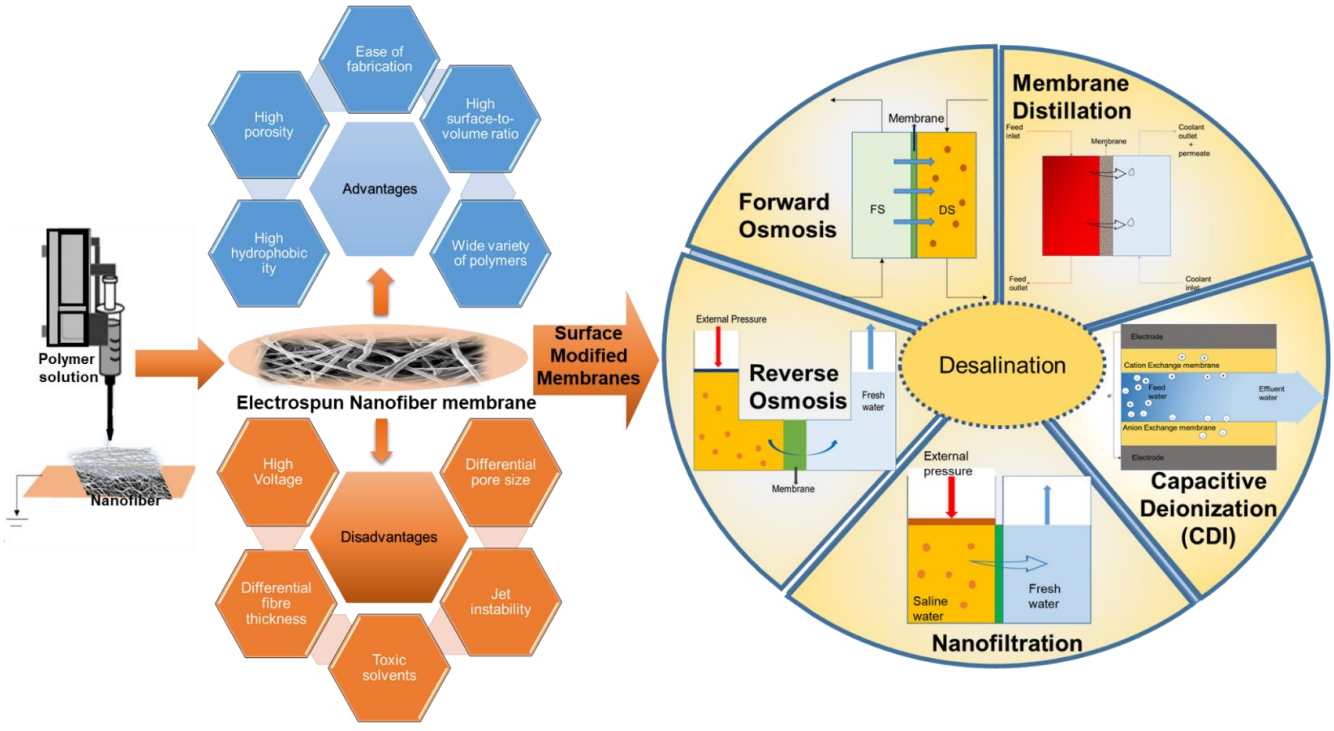

Figure 5. Nanofiber membrane advantages, disadvantages, and applications in desalination.

Table 2. Types of nanofiber membranes used for desalination of water.

Desalination Technology	Method	Types of Nanofiber Membrane and Modifications	Advantages and Separation Properties	References
Capacitive deionization (CDI)	Multistage controlled thermal treatment/electrospinning	Carbon nanofiber	High adsorption capacity	[76]
Membrane distillation	Fluorization/electrospinning	Carbon nanotube-modified nanofiber membrane	Improved water flux (49.3 kg/m^2–h) and hydrophobicity	[53]
	Electrospinning	PVDF–hexafluoropropylene (PVDF–HFP)-based nanofibers incorporated with Boron nitride nanosheets, carbon nanotubes, and coaxially electrospun membranes	Improved water flux, hydrophobicity, salt rejection (>99%), and liquid entry pressure (LEP)	[54–57]
		PVDF nanofibers functionalized with nano-additives (TiO_2, SiO_2, CuO, and MOF)	Enhanced membrane hydrophobicity, high salt rejection (>99%) and flux	[82]
		Superhydrophobic nanofiber membranes modified by surface fluorination, PTFE incorporation, CNT coating, polydimethylsiloxane (PDMS), and GO incorporation	Increased hydrophobicity, improved permeate flux, and high salt rejection (>99%)	[62,82–85]
		PVDF nanofiber membranes modified by MOF, nanoparticles, and fluorinated acrylate incorporation	Enhanced salt rejection (>99%), anti-fouling behavior, hydrophobicity, and outstanding mechanical properties	[82,86,87]
		Poly(vinyl alcohol) (PVA) incorporated with surfactant-based electrospun nanofibrous membranes	High pore volume, high water flux, and salt rejection (>99%)	[88]
		Omniphobic membranes	Increased hydrophobicity, porosity, flux (13.6 kg/m^2·h), and salt rejection (99%); stable performance	[89]
		Hydrophobic organosilica nanoparticle-doped nanofibers	Increased porosity and anti-fouling behavior	[90]
	Electrospinning/hot-pressing	Polystyrene-based nanofiber membrane	Enhanced water flux, high salt rejection (>99%), and cheap polymer availability	[49]
	Electrospinning/plasma treatment	CF_4 plasma-modified omniphobic electrospun nanofiber membrane	Improved flux (15.28 LMH), high salt rejection (~100%), and high potential in treating challenging feed solutions	[91]
	Electroblowing/hot-pressing	Styrene–acrylonitrile (SAN) nanofibrous membrane	High LEP, narrow pore size, high flux (50.8 kg/m^2·h), and high salt rejection (99%)	[92]
	Electrospinning/thermal rearrangement	Fluorine-containing thermally rearranged (TR) nanofiber membranes	Very high water flux (114.8 kg/m^2-h) and salt rejection (>99.99%); excellent energy efficiency and stable performance	[93,94]
	Melt blowing	Polypropylene nanofiber membrane	High-quality permeate water; membrane porosity >90% and high salt rejection >96%.	[95,96]

Table 2. *Cont.*

Desalination Technology	Method	Types of Nanofiber Membrane and Modifications	Advantages and Separation Properties	References
Forward osmosis	Electrospinning/interfacial polymerization	CA/PVDF nanofiber membrane via coaxial electrospinning	Very low specific reverse solute flux (0.03 g/L); higher flux (31.2 LMH) compared to PVDF TFC membrane.	[70]
		Polyacrylonitrile-based nanofiber TFC membrane	Enhanced water flux (16 LMH) and salt rejection	[71]
		Amorphous SiO_2 NP-incorporated poly(vinylidene fluoride) electrospun nanofiber membrane	Enhanced flux (83 LMH) and rejection (>99%)	[72]
Reverse osmosis	Electrospinning/interfacial polymerization	PAN thin-film nanofibrous composite	Increased permeate flux and high salt rejection (95%)	[66]
		Crosshatched nanofiber support modified by dopamine	Very high water flux (78 LMH) and salt rejection (98%)	[69]
	Interfacial polymerization	Cellulose nanofiber-based TFC nanocomposite	Enhanced water flux (29.8 LMH) and NaCl rejection (96.2%) compared to pristine RO membrane	[67,68]
Nanofiltration	Nonsolvent-induced phase separation/interfacial polymerization	Fabrication of composite polyamide/Kevlar aramid nanofiber	Stable membrane flux (14.4 LMH/bar) with excellent divalent salt rejection (>90%)	[74]

3.2. Heavy-Metal Remediation

To date, various technologies have been developed for the removal of heavy metals from wastewater, such as ion exchange, membrane filtration, electrochemical methods, and reverse osmosis [97]. However, these techniques require sophisticated instrumentation and sludge handling, while they are time-consuming and show low efficiency. Moreover, they cannot be used efficiently after more than few cycles [98]. In comparison, the adsorption technique provides a high yield of heavy-metal removal and regeneration of adsorbent, with affordable cost and sufficient options of adsorbents [99]. Nanofiber-based adsorbents are good candidates for heavy-metal ion removal compared to particle-based adsorbents [100]. Nanofibers have special structures with high surface area, high permeability, small pores with good interconnectivity, and the ability to change the functionality of fibers at the nanoscale [101]. Moreover, it is feasible to synthesize selective nanofibers depending upon target metal ion properties via the incorporation of specific functional groups, providing controllable diameter, porosity, and hydrophobicity, easier incorporation of additives, and practicability in creating the microstructure [102].

The basic mechanism that nanofibers follow to remove heavy metals from wastewater is adsorption, accompanied by ion exchange, photocatalytic process, electrostatic interaction between metal ions, diffusion dialysis, and metal–organic framework crystal or polymers [101,103]. Adsorption is viewed as a transfer progression of mass, in which heavy metals from wastewater get deposited on nanofibers by either physical adsorption or chemical adsorption. In physical adsorption, van der Waals forces favor multilayer adsorption, whereas, in chemical adsorption, chemical reactions take place on the adsorbent surface [104]. Firstly, heavy metals in the wastewater transfer to the surface of nanofibers and vice versa; then, from the exterior surface of nanofibers, heavy metals diffuse into the nanofibers, which is the rate-limiting step; finally, chemical/physical interactions occur between heavy metals and nanofibers [102,103]. The significant functional groups on the nanofiber surface selectively adsorbs the heavy metal, and equilibrium is achieved at a constant concentration of adsorbed heavy metals in wastewater. Langmuir and Freundlich's isotherm is the most common adsorption isotherm for studying equilibrium conditions [99].

Different studies have been focused on nanofiber fabrication with surface modification. Various absorbents are used in different forms such as metal oxides, polymers solution, zeolites, activated carbon, biomaterials, chelating materials, and functionalized chitosan, for the removal of heavy metals [104,105]. Nanofibers are fabricated using electrospinning, melt blowing, polymerization, melt blend extrusion, centrifugal force spinning, and phase separation [106]. Electrospinning was found to be the most versatile and straightforward method for the production of nanofibers by polymer solution with diameter ranges from hundreds of nanometers to microns [107]. Surface modification is done on electrospun fibers by doping, dispersion, crosslinking, and grafting with several compounds to enhance the adsorption capacity of nanofibers [108–110]. In this section, different types of nanofibers for heavy-metal removal are discussed. Cellulose nanofibers are green and biodegradable, extracted from sugarcane bagasse, and doping of nano MgS enables development into a bio-nano composite fiber with increased capacity toward Cd(II) [108]. Chitosan (CS) nanofibers are environmentally friendly because of their biodegradability, nontoxicity in nature, biocompatibility, low price, and higher abundance in nature. They strongly chelate with heavy metals because of the amine and hydroxyl groups in their polymeric structure [111]. Moreover, modifications have been done on CS nanofibers to improve their electrospinnability and enhance heavy-metal binding. Crosslinking between CS and PAAS (polyacrylic acid sodium) produced a homogeneously crosslinked chitosan structure with effective removal of Cr(VI) [111]. PEI grafted on the CS membrane improved the adsorption ability of heavy-metal ions [97]. Poly(vinyl alcohol) (PVA) is a water-soluble, nontoxic, biodegradable, high-strength, and biocompatible molecule, with high capability of fiber formation (Ortiz, 2018) [98]. The mixture of two water-soluble polymers,

PVA and sodium alginate (SA), was used to fabricate a composite nanofiber through electrospinning and the creation of crosslinks through thermal crosslinking for the removal of Cd(II) from aqueous solution [109]. The polymer resins used for nanofiber preparation are thermoplastic polyolefins or polyesters, which can be melted and processed again. A nanofiber of poly(vinyl alcohol-*co*-ethylene) (PVA-*co*-PE) was prepared by melt extrusion and functionalized with iminodiacetic acid for the removal of Cu(II) [112]. Poly(ethylene-*co*-vinyl alcohol) EVOH nanofiber was functionalized with polypyrrole (PPy) by in situ oxidative polymerizations for the removal of Cr(VI) from an aqueous solution [112]. PAN is a synthetic polymer used for making nanoscopic fibrous materials by electrospinning. It incorporates amidoxime, hydrazine, amine, and phosphoryl as its functional groups, allowing chelation with heavy metals [98]. Three types of nanostructured PAN nanofiber were fabricated by chemical grafting of diethylenetriamine (DTA), ethylenediamine (EDA), and ethylene glycol (EG) on the PAN surface for the removal of Zn (II), Cu (II), and Pb (II) [110].

Yang et al. (2019) [97] successfully prepared a CS–PGMA–PEI electrospun membrane, which showed maximum adsorption capacities for Cr(VI), Cu(II), and Co(II) of 138.96 mg/g, 69.27 mg/g, and 68.31 mg/g at an optimum pH of 2, 4, and 6, respectively. It showed higher adsorption competition of Cr(VI) with respect to Co(II) and Cu(II). Uniform distribution was obtained for Cr(VI), Cu(II), and Co(II) over the electrospun nanofiber. Moreover, there was a decrement in adsorption capacities after five adsorption–desorption cycles by 17.80%, 11.30%, and 13.50% for Cr(VI), Cu(II), and Co(II), respectively. By contrast, the adsorption capacity of CS/PAAS nanofibers for Cr(VI) was 26.02 mg/g and increased to 78.92 mg/g on post-modification with chelating agents, which enhanced its chelating abilities [111]. MgS-doped cellulose nanofibers showed excellent adsorption and reproducibility of Cd(II), with a maximum adsorption capacity of 333.33 mg/g. The pH changes showed that cadmium removal highly depends on solution pH, contributing to the complexing of Cd(II) and OH^- groups of cellulose to form cadmium hydroxide. Increasing pH from 5 to 5.5 enhanced cadmium removal by 17%, and further increment decreased the adsorption by around 40% [108]. Ebrahimi et al. (2019) [109] prepared PVA/SA nanofibers which exhibited higher Cd(II) adsorption capacity up to 163.9344 mg/g at 120 mg/L cadmium concentration. By contrast, the sulfhydryl-modified PVA/TiO_2 exhibited adsorption capacity for Th(VI) up to 238.1 mg/g, and the introduction of ZnO into the system enhanced the adsorption capacity of PVA/TiO_2/ZnO to 333.3 mg/g [113,114]. Mesoporous MgO nanofibers were fabricated by electrospinning with deposition of PPG (polypropylene glycol) on the surface of nanofibers. The result showed that MgO/PPG nanofibers had very high adsorption capacities for Pb(II), Cd(II), and Cu(II) up to 2500.48, 2407.74, and 2415.74 mg/g, respectively, compared to the mesoporous MgO nanofiber adsorption capacities of 378.58, 311.47, and 270.11 mg/g respectively [105]. Researchers prepared zonal silica nanofibers via the dissolution of PAN templates with DMF for the removal of Hg^{2+}, which showed an adsorption capacity of 77.49 mg/g, whereas purely silica nanofibers exhibited a lower adsorption capacity of 1.36 mg/g [100]. The key results of heavy-metal removal by nanofibers are summarized in Table 3.

Table 3. A summary of heavy-metal remediation using nanofibers.

Nanofiber Type	Methodology	Adsorption Capacity (mg/g)	Heavy Metals Ion	Functional Group	Adsorbent Dose (g/L)	pH	Equilibrium Time (h)	Isotherm	Removal %	Ref.
Zonal silica nanofiber	Electrospinning with MTPS coating	57.49	Hg(II)	Sulfhydryl			1			[100]
Carbon nanofiber	Polymerization, functionalization, and magnetization	375.9	Cu(II)	Carboxyl	0.5	6	1	Langmuir	99.5	[115]
PVA/SA nanofibers	Electrospinning with thermal crosslinking	93.163	Cd(II)	Carboxyl	0.13	5	1.67	Langmuir		[109]
MgS/cellulose nanofiber	Mechanical fibrillation with doping	333.33	Cd(II)	Sulfinyl	0.5	5.5	16	Langmuir	94.5	[108]
Titanate nanofibers	Pyrochemical process	244.26	Pb(II)	–O–Ti	0.4	7	48			[116]
EVOH/PPy nanofiber	Melting blend extrusion with polymerization	90.74	Cr(VI)	Amine	3.3	2	8	Langmuir	90	[106]
CS/PGMA/PEI nanofiber	Electrospinning with grafting	138.96, 69.27, 68.31	Cr(VI), Cu(II), Co(II)	Amine	0.3	2, 4, 6	1	Langmuir	80, 40, 30	[97]
MgO/PPG nanofiber	Electrospinning with functionalization	2377.75, 2280.5, 2181.75	Pb(II), Cu(II), Cd(II)	Amide	0.1	7.5	1	Langmuir	98, 92, 90	[105]
CS/PAAS nanofiber	Electrospinning with crosslinking	26.02	Cr(VI)	Carboxyl	0.67	3	48	Langmuir		[111]
PAN nanofiber	Electrospinning with chemical grafting	33.44, 1250, 769.23	Cu(II), Pb(II), Zn(II)	Carboxyl	2	6	2	Langmuir	90	[110]

Nanofibers for the removal of heavy metals from wastewater are discussed in this section. A comparison was drawn among various nanofibers with respect to their fabricating method, dose of nanofiber, functional groups, and adsorption capacity. The functional group on the adsorbent surface controls the ion selectivity and adsorption capacity. The pH of the solution majorly influences the metal remediation. Low adsorbent dose and operation cost, high adsorption/regeneration efficiency, and ecofriendly extraction make nanofibers economically suitable. Currently, nanofiber fabrication takes a long time with a low yield at the pilot scale. More research studies are needed for nanofiber mass production with higher yield for its usage at the industrial level. The changes introduced in the polymeric solution by introducing inorganic materials make the spinning process quite unstable. Hence, further research with more efficient spinning technology needs to be done. Industrial wastewater is the primary source of heavy metals, which is complexed with highly corrosive and acidic/basic substances. Therefore, the development of acid/base-resistant nanofibers is needed. Moreover, research studies in developing mechanically stable, strong, and reusable nanofibers are recommended. Current studies mainly focus on static and single metal ion removal via nanofibers, whereas wastewater is composed of complex heavy-metal ions. Hence, studies in the field of dynamic adsorption and selective adsorption of heavy metals need to be improved.

3.3. CEC Removal

Contaminants of emerging concern (CECs) are largely pollutants of anthropogenic origin detected in trace concentrations (from ng/L to µg/L) in our water systems but not typically monitored. Lab studies show that these chemicals can cause adverse ecological and/or human health effects. However, assessing the actual damage caused by them under realistic scenarios would take some years to manifest. Therefore, environmental regulatory agencies have started to update their monitoring and treatment protocols periodically. These contaminants are largely released from agricultural pesticides, veterinary pharmaceuticals, pharmaceuticals, personal care, and household products into the environment [117].

Due to their low concentrations and conventional treatment systems, which were not designed for their removal, CECs have been reported even in the treated water from wastewater treatment plants (WWTPs) [118], drinking water treatment plants (DWTPs), and household supply water [119]. The long-term consumption of such water containing CECs is a serious health risk; therefore, many studies have been carried out for their removal. The key challenges to their removal include their low concentrations in the water systems, high concentrations of their background matrix, and conventional centralized treatment methods not designed for CEC-specific removal. These challenges have spurred numerous studies exploring CEC removal using various physicochemical treatment technologies such as adsorption, advanced oxidation processes (AOPs), electrochemical oxidation, and membrane-based schemes. In this context, the available literature suggests that nanofiber-based approaches have been quite versatile, incorporating one or more of the abovementioned physicochemical treatment schemes.

Nanofibers have been utilized as adsorbents for CECs. However, since they can immobilize the target contaminants in their polymeric matrix via adsorption, they can also be used for targeted localized oxidation via AOPs or electrochemical methods after adsorbing the contaminants. The tunable character of nanofibers allows them to be specifically functionalized with various functionals groups, catalysts, and chemical additives that possess high selectivity for the target CECs, which would facilitate their removal from trace-concentration aqueous samples with a high-concentration background matrix. Another advantage of nanofibers is that they can be used in cases where dispersing remediating agents in the aqueous media is difficult as in nanoparticle adsorbents/catalysts that run the risk of agglomeration and high turbidity, particularly for UV-based AOPs. Secondly, water treatment using nanoparticles also suffers from the limitation of recovering nanoparticles from the aqueous media after the process is completed. Incorporating nanoparticles in

nanofibers can address this issue of their final recovery. Moreover, their regeneration can be performed, and the nanoparticles can be reused in a multiple cycle operation. Additionally, when it comes to immobilizing macrocyclic hosts such as cyclodextrins (CD), the high surface area and permeability of nanofibers make them an ideal substrate as they can accommodate a large quantity of these molecules, which aid in CEC removal by adsorption. For CECs, which are in trace concentration in the water samples, their adsorption over nanofibers also increases their localized concentration. Therefore, it leads to highly efficient localized and targeted treatment using oxidation processes such as AOPs and electrochemical or plasma treatment systems.

Several studies have reported the applications of nanofibers for treating CECs using standalone adsorption or adsorption in conjunction with catalytic, electrochemical, or plasma oxidation of the adsorbed CECs. Camiré et al. (2020) [120] investigated the removal of fluoxetine using nanofibers synthesized from alkali lignin (AL) and polyvinyl alcohol (PVA) solutions. The study estimated different ratios of AL and PVA. It established that, at 50:50 AL:PVA, maximum removal (70%) of fluoxetine from its 50 mg/L solutions was observed in a batch system with hydrogen bonding as the dominant removal mechanism. Incorporating lignin in PVA showed a reduction in the solution viscosity, which required a lower flow rate during the electrospinning process to sustain nanofiber synthesis. Ultimately, this implied longer electrospinning time and higher operating costs. The stability of the nanofibers in the aqueous solution was another issue, as the lignin nanofibers dissolved in the water showed the characteristic yellow-brown color of lignin. Therefore, thermo-stabilization is needed, which can further add to the overall cost of the system. Peter et al. (2016) [121] electrospun a carbon nanofiber (CNF)–carbon nanotube (CNT) composite to remove atrazine and sulfamethoxazole at 50 µM concentration by adsorption from aqueous solutions. Ten more CECs at 5 µg/L concentration each were also studied for their removal by the nanofibers. The CNF without CNTs showed poor adsorption; however, with the incorporation of CNTs, the specific surface area and mechanical strength of the nanofibers increased, and higher uptake capacity and faster kinetics were observed. The nanofiber average diameter without CNTs was reported as 160 nm; however, with their incorporation, the diameter reduced to 100 nm, ultimately resulting in a higher specific surface area. The decrease in diameter was attributed to the higher conductivity due to CNT–CNF sol–gel. The nanofiber showed >90% removal for all the CECs in a flowthrough system with 30 mg/g and 20 mg/g as the uptake capacities of atrazine and sulfamethoxazole, respectively. Chabalala et al. (2021) [122] investigated PAN nanofiber modification with β-cyclodextrin (β-CD) to enhance the percentage removal of 10 mg/L atrazine from 51% for PAN nanofibers to 91.46% for PAN–CD nanofibers. The enhanced removal was reported to be caused due to the increased specific surface area (the average diameter was reduced to 497 nm for PAN–CD nanofibers compared to 557 nm for PAN nanofibers) and intermolecular interaction and complexation between atrazine and incorporated β-CD in PAN–CD nanofibers. In another study utilizing β-CD, Lv et al. (2021) [123] modified cellulose nanofibers incorporating β-CD to remove bisphenol A (BPA), bisphenol S (BPS), and bisphenol F (BPF). The factors affecting adsorption included adsorbent dosage, temperature, and pH, and the maximum uptake capacities for BPA, BPS, and BPF were 50.37 mg/g. 48.52 mg/g, and 47.25 mg/g, respectively, at 0.1 g/L adsorbent dose, pH 7, and a temperature of 25 °C. The removal mechanism included the synergistic effects of hydrophobic interaction, hydrogen bonding, and π–π interaction. The study also investigated BPA, BPS, and BPF (all at 0.5 mg/L) removal from lake and river water samples. The nanofibers also showed reuse potential up to five cycles after desorption using a water and ethanol mixture at 10/90 (v/v). Khalil and Schäfer (2021) [124] investigated polyethersulfone (PES) nanofibers with β-CD deposited over PES UF membranes. β-CD is a soluble polysaccharide; therefore, to incorporate it within the polymeric matrix, a crosslinking agent such as epichlorohydrin was used. The study demonstrated the removal of steroid hormones (estrone, β-estradiol, and testosterone) found in aqueous samples at concentrations less than 100 ng/L. The steroids showed removal via size exclusion based

on the diameter of the opening of the β-CD cavity and the size of the steroids. Khalil et al. (2021) [125] studied the role of β-CD crosslinking agents such as epichlorohydrin, trimethylolpropane triglycidyl ether (TPTE), and triphenylmethane triglycidyl ether (TMTE) in the removal of estradiol. The nanofibers with TPTE as crosslinker showed the highest (95%) removal of 10 ng/L–100 µg/L estradiol in 5 h.

Several studies have utilized nanofibers for first adsorbing and then subsequently degrading the CECs using photocatalysts immobilized in the nanofiber matrix. Nor et al. (2016) [126] hot-pressed TiO_2 nanofibers onto a polyvinylidene difluoride (PVDF) membrane used as support. The study demonstrated 63–85% degradation of 10 mg/L BPA through the photocatalytic behavior of TiO_2 using a UV light source (312 nm, 30 W, 1.45 mW/cm^2 light intensity). Without photocatalysis, a maximum of 27.62% removal was observed due to adsorption alone. Gadisa et al. (2020) [127] examined ZnO–carbon composite nanofibers for 30 mg/L caffeine removal. The study investigated different polymeric precursors (PAN, polystyrene (PS), and polyvinyl pyrrolidone (PVP)) for nanofiber synthesis via electrospinning to determine their effect on charge carrier properties, and they demonstrated that carbon doping efficiency varied with the precursors and determined their photocatalytic activities. Caffeine removal was the fastest and highest for ZnO–PS achieving 80.4% photodegradation in 2 h; diclofenac showed 79.5% removal within that period. Ramasundaram et al. (2013) [128] studied cimetidine removal using a photocatalytic stainless-steel filter where TiO_2 nanofibers were hot-pressed over the metal filter with PVDF as a binder in between. In this study, 90% removal of cimetidine was observed at 10 LMH flux with the nanofiber layer thickness governing the removal process. The removal increased from 40% to 90% by increasing the TiO_2 nanofiber layer thickness from 10 µm to 29 µm; beyond 29 µm, no increase in the removal was noticed. Chen et al. (2021) [129] studied hollow and porous Fe-doped PAN nanofibers for activating peroxymonosulfate (PMS) for achieving the removal of BPA. Electrospinning showed high effectiveness in immobilizing the nanoparticles by suppressing the agglomeration of nanoparticles and facilitating a uniform dispersion of nanoparticles, leading to an increase in catalytic sites. BPA was first adsorbed over the nanofibers, and then PMS was added to initiate the degradation. The synergistic impact of adsorption and oxidation by PMS resulted in 100% BPA removal in 6 min. PAN nanofibers with TiO_2 nanoparticles dispersed in the polymeric matrix were investigated to remove a host of CECs (atrazine, benzotriazole, caffeine, carbamazepine, DEET, metoprolol, naproxen, and sulfamethoxazole) each at 0.5 µM concentration [130]. Phthalic acid was used as a dispersant of nanoparticles, and its optimum dosing was estimated for nanofiber morphology and removal capacity. Phthalic acid increased the diameter of nanofibers and introduced porosity due to increased viscosity and volatilization, respectively. The nanofiber was able to remove 90% of all the CECs in a flowthrough system.

The use of nanofibers in electrochemical systems has been shown to achieve CEC remediation in the available literature. Kim et al. (2019) [131] studied antimony tin oxide-doped ruthenium oxide (ATO-RO) nanoparticles incorporated into PVP nanofibers. The nanofiber was subsequently utilized as the anode material for electrochemical oxidation of BPA at a concentration of 0.25 mM and showed complete degradation of the CEC by 20 min of electrolysis at 3 mA/cm^2 current density. Xie et al. (2021) [132] investigated Fe/Co alloy on PVP nanofibers for the degradation of 30 mg/L, 40 mg/L, and 50 mg/L tetracycline solutions. The degradation values reported were 100%, 93.12%, and 88.38% for 30 mg/L, 40 mg/L and 50 mg/L solutions, respectively. Yang and Hen (2013) [133] examined tubular carbon nanofibers with activated alumina over PVC support as the anode material for an electrocoagulation system. The system removed 95.8% of caffeine, 94.9% of sulfamethoxazole, and 79.8% of acetaminophen, all at 200 µg/L initial concentration. A summary of CEC removal by nanofibers is presented in Table 4.

Table 4. A summary of CEC remediation using nanofibers.

Nanofiber Type	CECs Removed	CEC Removal Experimental Conditions	Removal %/Uptake Capacity	Removal Mechanism	Remarks	Reference
Alkaline lignin (AL) in PVA	Fluoxetine	50 ppm fluoxetine in citrate buffer pH 4.5 solution; batch system (2–5 h shaking)	70%	Adsorption with H-bonding	50:50 AL:PVA mass ratio nanofibers showed the best removal; stability of nanofibers was an issue in the solution	[120]
Fe/Co alloy on carbon nanofibers (PVP)	Tetracycline (TC)	30 mg/L TC in 1 M Na_2SO_4 at pH 5 used as electrolyte with current at 3 mA	100% at 30 mg/L TC, 93.12% for 40 mg/L TC, and 88.38% for 50 mg/L TC	Adsorption on the nanofiber-based anode followed by electrochemical degradation	Faradaic efficiency decreased with TC concentration; 81.29% efficiency in the first 2 h reduced to 26.13% for complete removal after 12 h; the power consumption varied from 6.17 kWh/kg to 19.2 kWh/kg; the electrode was recycled 10 times	[132]
PAN nanofibers modified by β-CD crosslinked by citric acid	Atrazine	Atrazine concentrations between 5 and 25 ppm with an adsorbent dosage between 0.033 and 0.336 g, pH between 2 and 12, and contact time between 60 and 360 min were studied	Max removal of 91.46% was reported at an atrazine concentration of 10 mg/L	Adsorption and complexation by β-CD	Incorporation of β-CD into the nanofiber reduced the nanofiber diameter from 557 nm to 497 nm and enhanced the surface roughness	[122]
β-CD modified cellulose nanofibers	BPA, BPS, BPF	Two real water samples from local lakes with 0.5 ppm each of BPA, BPF, and BPS	100% removal for treating up to 0.58 L of water samples in a flow membrane filtration system	Adsorption with synergistic effects of hydrophobic interaction, hydrogen bonding, and π–π interaction	The study also performed a desorption study using water and methanol in 10:90 *v*/*v* ratio for 2 h and demonstrated 5 cycles of regeneration	[123]
Fe/N-doped PAN nanofibers	BPA	20 mg/L, 30 mg/L, and 40 mg/L BPA, pH 3–9, 0.2–0.4 g/L nanofiber dosage	100% removal in 6 min for 20 mg/L BPA	Adsorption followed by degradation with PMS	The nanofibers were carbonized, and BPA removal correlated with carbonation temperature directly in the range of 700–900 °C	[129]
PAN–CNT composite nanofibers	Atrazine, sulfamethoxazole, and 10 other CECs	Adsorbent dosage 0.5 g/L, pH ~7, atrazine and sulfamethoxazole each at 50 μM, and other 10 CECs each at 5 μg/L	>90% removal for the CECs with breakthrough volume varying among CECs	Adsorption by CNTs with PTA induced macro porosity, making CNTs accessible to CECs	The removal is pH-dependent; PTA encouraged macroporosity in the nanofibers, making CNTs accessible to the CECs; however, too much microporosity could hamper the material strength of the nanofibers	[121]

Table 4. *Cont.*

Nanofiber Type	CECs Removed	CEC Removal Experimental Conditions	Removal %/Uptake Capacity	Removal Mechanism	Remarks	Reference
ZnO–carbon composite nanofibers	Caffeine, diclofenac	30 mg/L caffeine in 30 mL solution with 30 mg of the nanofibers, 30 min of adsorption followed by UV irradiation	80.4% caffeine degradation by ZnO–PS nanofibers in 120 min; 79.5% degradation for diclofenac in 2 h	Adsorption followed by UV degradation; hydroxyl radicals were the most active species responsible for the CEC degradation	ZnO doped in various polymeric pre-cursor nanofiber matrices (PAN, PS, PVP); best degradation obtained for ZnO–PS nanofibers; doping introduced new energy levels that lowered band gap energy by 0.35 eV	[127]
PES nanofibers with β-CD–epichlorohydrin (crosslinker) deposited over PES UF membranes	Steroid hormones (estrone, β-estradiol, testosterone)	Hormone concentration varied between 10 ng/L and 1 mg/L with background of 1 mM $NaHCO_3$ and 10 mM NaCl	80% removal in 5 h for static removal; 99% removal reported for dynamic system	Size exclusion based on the diameter of β-CD cavity and size of the hormones	The hormone removal depended on the hormonal concentration, pH of the solution, contact time, β-CD concentration in the nanofibers, hormone type, and flow rate	[124]
TiO_2 nanoparticles immobilized in polyamide nanofiber	Isoproturon	5 mg/L and 10 mg/L isoproturon solutions irradiated with UV light at 5 mW/cm^2 intensity	100% degradation	Adsorption followed by photodegradation	Isoproturon degradation increased with increasing TiO_2 concentration in polyamide nanofibers	[119]
TiO_2 nanoparticles immobilized in PAN nanofiber	Atrazine, benzotriazole, caffeine, carbamazepine, DEET, naproxen, metoprolol, sulfamethoxazole	All CECs were at 0.5 μM in the background of dissolved organic matter and carbonate alkalinity	40–90% removal in a single-pass flowthrough system with UV irradiation	Crossflow filtration with simultaneous UV irradiation	2.5% phthalic acid was used as a dispersant of TiO_2 nanoparticles, which increased the diameter of the nanofibers and also introduced pores and flexibility due to volatilization	[130]

Most of the studies reported in the literature have not investigated the application of nanofibers for CEC remediation in a realistic system where co-contaminants are majorly present and can easily foul or degrade the sorption sites on the nanofibers. Additionally, the components present in the background matrix will also compete with the CECs for the sorption sites. Since CECs are present in trace concentration, the co-contaminants are more likely to be removed by the nanofibers than the CECs. In the case of photocatalytic systems, the turbidity of the background matrix can also impact the process efficiency. Therefore, more studies should be conducted to analyze the role of the background matrix and characterize and improve the selectivity of the nanofibers. In electrochemical systems, the biggest challenge is maintaining the current efficiency at lower CEC concentrations in line with that at higher concentrations. Most studies demonstrated the feasibility of electrochemical systems at much higher levels of CECs than naturally found in water systems. High energy consumption is also a limitation of electrocatalytic degradation. A nanofiber anode-based electrochemical system showed 81.29% current efficiency and power consumption of 6.16 kWh/kg within the first 2 h of the electrolysis. At a low concentration of the CEC, the efficiency dropped to 26.13%, with a power consumption of 19.2 kWh/kg after 12 h of operation [132]. Maintaining a consistent current efficiency and power consumption within a narrow range is a challenge for nanofiber-based anode materials that should be addressed. Another aspect of nanofibers, in general, is their reusability and final disposal. Both of these aspects remain largely unaddressed in the available literature.

4. Conclusions

Nanofibers are versatile and tunable nanomaterials that have diverse environmental applications, including air filtration, water filtration, and contaminant abatement. Their wide range of application stems from the flexibility of process parameters in the synthesis using electrospinning. By controlling the process, nanofibers with a desirable set of properties can be obtained, and specific and nonspecific remediation schemes can be developed. Nanofibers can be utilized as adsorbents, photocatalysts, electrodes, and membranes. Therefore, they are amenable to treating different kinds of water samples and streams. In desalination applications, nanofiber-based MD processes are among the most widely used techniques. The tunable hydrophobicity of nanofibers provides excellent pore wettability and control over the process. In RO processes, nanofiber-based membranes have shown excellent salt rejection and water flux with better anti-fouling properties. Nanofibers with a high surface-area-to-volume ratio, uniform pore distribution, and improved pore connectivity make them useful for desalination applications. For heavy-metal remediation, nanofibers have been largely utilized as adsorbents, and they have exhibited high selectivity for the target heavy metals in the presence of background matrix. For application as adsorbents for heavy-metal or CEC removal, nanofibers require functional groups in their polymeric matrix, which have selectivity for the target contaminants. Nanofibers with a high specific surface area can incorporate these specific groups efficiently and can help in the removal of the contaminants, further facilitating their removal/degradation using photocatalytic or electrochemical degradation. One of the key drawbacks of nanofibers is their large-scale production and scaling up of the electrospinning process. Moreover, the final disposal of the exhausted nanofibers needs to be explored in detail. Process efficiency issues (regeneration, recyclability, and role of background matrix) should be addressed in future studies, specifically for removing/degrading contaminants reported in trace concentrations.

Author Contributions: Conceptualization, T.N., S.P.S., T.S. and A.R. writing—original draft preparation, S.A., R.R., B.L., S.P.S. and T.N.; writing—review and editing, S.A., R.R., B.L., S.P.S., A.R., T.S. and T.N.; supervision, S.P.S., A.R., T.S. and T.N.; funding acquisition, S.P.S., A.R., T.S. and T.N. All authors have read and agreed to the published version of the manuscript.

Funding: This research received no external funding.

Acknowledgments: We gratefully acknowledge the Indian Institute of Technology Bombay (IIT Bombay) for their support of this work.

Conflicts of Interest: The authors declare no conflict of interest.

References

1. Ahn, Y.; Park, S.; Kim, G.; Hwang, Y.; Lee, C.; Shin, H.; Lee, J. Development of high efficiency nanofilters made of nanofibers. *Curr. Appl. Phys.* **2006**, *6*, 1030–1035. [CrossRef]
2. Lannutti, J.; Reneker, D.; Ma, T.; Tomasko, D.; Farson, D. Electrospinning for tissue engineering scaffolds. *Mater. Sci. Eng. C* **2007**, *27*, 504–509. [CrossRef]
3. Hunley, M.T.; Long, T.E. Electrospinning functional nanoscale fibers: A perspective for the future. *Polym. Int.* **2008**, *57*, 385–389. [CrossRef]
4. Reneker, D.H.; Yarin, A.L. Electrospinning jets and polymer nanofibers. *Polymer* **2008**, *49*, 2387–2425. [CrossRef]
5. Kenry; Lim, C.T. Nanofiber technology: Current status and emerging developments. *Prog. Polym. Sci.* **2017**, *70*, 1–17. [CrossRef]
6. Vasita, R.; Katti, D.S. Nanofibers and their applications in tissue engineering. *Int. J. Nanomed.* **2006**, *1*, 15–30. [CrossRef]
7. Benelli, G.; Pavela, R.; Maggi, F.; Petrelli, R.; Nicoletti, M. Commentary: Making Green Pesticides Greener? The Potential of Plant Products for Nanosynthesis and Pest Control. *J. Clust. Sci.* **2017**, *28*, 3–10. [CrossRef]
8. Fortunati, E.; Peltzer, M.A.; Armentano, I.; Torre, L.; Jiménez, A.; Kenny, J.M. Effects of modified cellulose nanocrystals on the barrier and migration properties of PLA nano-biocomposites. *Carbohydr. Polym.* **2012**, *90*, 948–956. [CrossRef] [PubMed]
9. Ramakrishna, S.; Fujihara, K.; Teo, W.E.; Lim, T.C.; Ma, Z. *An Introduction to Electrospinning and Nanofibers*; World Scientific: Singapore, 2005. [CrossRef]
10. Bhardwaj, N.; Kundu, S.C. Electrospinning: A fascinating fiber fabrication technique. *Biotechnol. Adv.* **2010**, *28*, 325–347. [CrossRef] [PubMed]
11. Pan, Y.; Zeng, L. Simulation and Validation of Droplet Generation Process for Revealing Three Design Constraints in Electrohydrodynamic Jet Printing. *Micromachines* **2019**, *10*, 94. [CrossRef]
12. Bonura, L.; Bianchi, G.; Ramirez, D.O.S.; Carletto, R.A.; Varesano, A.; Vineis, C.; Tonetti, C.; Mazzuchetti, G.; Lanzarone, E.; Ortelli, S.; et al. Monitoring Systems of an Electrospinning Plant for the Production of Composite Nanofibers. In *Factories of the Future*; Springer: Cham, Switzerland, 2019; pp. 315–337.
13. Rodoplu, D.; Mutlu, M. Effects of Electrospinning Setup and Process Parameters on Nanofiber Morphology Intended for the Modification of Quartz Crystal Microbalance Surfaces. *J. Eng. Fibers Fabr.* **2012**, *7*, 155892501200700. [CrossRef]
14. Jacobs, V.; Anandjiwala, R.D.; Maaza, M. The influence of electrospinning parameters on the structural morphology and diameter of electrospun nanofibers. *J. Appl. Polym. Sci.* **2010**, *115*, 3130–3136. [CrossRef]
15. Sukigara, S.; Gandhi, M.; Ayutsede, J.; Micklus, M.; Ko, F. Regeneration of Bombyx mori silk by electrospinning—Part 1: Processing parameters and geometric properties. *Polymer* **2003**, *44*, 5721–5727. [CrossRef]
16. Deitzel, J.; Kleinmeyer, J.; Harris, D.; Tan, N.B. The effect of processing variables on the morphology of electrospun nanofibers and textiles. *Polymer* **2001**, *42*, 261–272. [CrossRef]
17. McKee, M.G.; Wilkes, G.L.; Colby, A.R.H.; Long, T.E. Correlations of Solution Rheology with Electrospun Fiber Formation of Linear and Branched Polyesters. *Macromolecules* **2004**, *37*, 1760–1767. [CrossRef]
18. Haghi, A.K.; Akbari, M. Trends in electrospinning of natural nanofibers. *Phys. Status Solidi A* **2007**, *204*, 1830–1834. [CrossRef]
19. Williams, G.R.; Raimi-Abraham, B.T.; Luo, C.J. Electrospinning fundamentals. In *Nanofibres in Drug Delivery*; UCL Press: London, UK, 2018; pp. 24–59. [CrossRef]
20. Buchko, C.J.; Chen, L.C.; Shen, Y.; Martin, D. Processing and microstructural characterization of porous biocompatible protein polymer thin films. *Polymer* **1999**, *40*, 7397–7407. [CrossRef]
21. Shenoy, S.L.; Bates, W.D.; Frisch, H.L.; Wnek, G.E. Role of chain entanglements on fiber formation during electrospinning of polymer solutions: Good solvent, non-specific polymer–polymer interaction limit. *Polymer* **2005**, *46*, 3372–3384. [CrossRef]
22. Kameoka, J.; Orth, R.; Yang, Y.; Czaplewski, D.; Mathers, R.; Coates, G.W.; Craighead, H.G. A scanning tip electrospinning source for deposition of oriented nanofibres. *Nanotechnology* **2003**, *14*, 1124–1129. [CrossRef]
23. Zong, X.; Kim, K.; Fang, D.; Ran, S.; Hsiao, B.S.; Chu, B. Structure and process relationship of electrospun bioabsorbable nanofiber membranes. *Polymer* **2002**, *43*, 4403–4412. [CrossRef]
24. Demir, M.M.; Yilgor, I.; Yilgor, E.; Erman, B. Electrospinning of polyurethane fibers. *Polymer* **2002**, *43*, 3303–3309. [CrossRef]
25. Deitzel, J. Electrospinning of polymer nanofibers with specific surface chemistry. *Polymer* **2002**, *43*, 1025–1029. [CrossRef]
26. Doshi, J.; Reneker, D.H. Electrospinning process and applications of electrospun fibers. *J. Electrost.* **1995**, *35*, 151–160. [CrossRef]
27. Zeng, J.; Xu, X.; Chen, X.; Liang, Q.; Bian, X.; Yang, L.; Jing, X. Biodegradable electrospun fibers for drug delivery. *J. Control. Release* **2003**, *92*, 227–231. [CrossRef]
28. Lasprilla-Botero, J.; Alvarez-Lainez, M.; Lagaron, J. The influence of electrospinning parameters and solvent selection on the morphology and diameter of polyimide nanofibers. *Mater. Today Commun.* **2018**, *14*, 1–9. [CrossRef]
29. Son, W.K.; Youk, J.H.; Lee, T.S.; Park, W.H. Electrospinning of ultrafine cellulose acetate fibers: Studies of a new solvent system and deacetylation of ultrafine cellulose acetate fibers. *J. Polym. Sci. Part B Polym. Phys.* **2004**, *42*, 5–11. [CrossRef]
30. Choi, J.S.; Lee, S.W.; Jeong, L.; Bae, S.-H.; Min, B.C.; Youk, J.H.; Park, W.H. Effect of organosoluble salts on the nanofibrous structure of electrospun poly(3-hydroxybutyrate-co-3-hydroxyvalerate). *Int. J. Biol. Macromol.* **2004**, *34*, 249–256. [CrossRef]

31. Lu, C.; Chen, P.; Li, J.; Zhang, Y. Computer simulation of electrospinning. Part I. Effect of solvent in electrospinning. *Polymer* **2006**, *47*, 915–921. [CrossRef]
32. Veleirinho, B.; Rei, M.F.; Lopes-Da-Silva, J.A. Solvent and concentration effects on the properties of electrospun poly(ethylene terephthalate) nanofiber mats. *J. Polym. Sci. Part B Polym. Phys.* **2008**, *46*, 460–471. [CrossRef]
33. Wu, X.; Wang, L.; Yu, H.; Huang, Y. Effect of solvent on morphology of electrospinning ethyl cellulose fibers. *J. Appl. Polym. Sci.* **2005**, *97*, 1292–1297. [CrossRef]
34. Luo, C.; Nangrejo, M.; Edirisinghe, M. A novel method of selecting solvents for polymer electrospinning. *Polymer* **2010**, *51*, 1654–1662. [CrossRef]
35. Wu, X.-F.; Salkovskiy, Y.; Dzenis, Y.A. Modeling of solvent evaporation from polymer jets in electrospinning. *Appl. Phys. Lett.* **2011**, *98*, 223108. [CrossRef]
36. Zhao, S.; Wu, X.; Wang, L.; Huang, Y. Electrospinning of ethyl-cyanoethyl cellulose/tetrahydrofuran solutions. *J. Appl. Polym. Sci.* **2004**, *91*, 242–246. [CrossRef]
37. Zhang, C.; Yuan, X.; Wu, L.; Han, Y.; Sheng, J. Study on morphology of electrospun poly(vinyl alcohol) mats. *Eur. Polym. J.* **2005**, *41*, 423–432. [CrossRef]
38. Yuan, X.; Zhang, Y.; Dong, C.; Sheng, J. Morphology of ultrafine polysulfone fibers prepared by electrospinning. *Polym. Int.* **2004**, *53*, 1704–1710. [CrossRef]
39. Zuo, W.; Zhu, M.; Yang, W.; Yu, H.; Chen, Y.; Zhang, Y. Experimental study on relationship between jet instability and formation of beaded fibers during electrospinning. *Polym. Eng. Sci.* **2005**, *45*, 704–709. [CrossRef]
40. Laurencin, C.; Kumbar, S.; Nukavarapu, S.; James, R.; Hogan, M. Recent Patents on Electrospun Biomedical Nanostructures: An Overview. *Recent Pat. Biomed. Eng.* **2008**, *1*, 68–78. [CrossRef]
41. Reneker, D.H.; Yarin, A.L.; Fong, H.; Koombhongse, S. Bending instability of electrically charged liquid jets of polymer solutions in electrospinning. *J. Appl. Phys.* **2000**, *87*, 4531–4547. [CrossRef]
42. Ki, C.S.; Baek, D.H.; Gang, K.D.; Lee, K.H.; Um, I.C.; Park, Y.H. Characterization of gelatin nanofiber prepared from gelatin–formic acid solution. *Polymer* **2005**, *46*, 5094–5102. [CrossRef]
43. Mit-Uppatham, C.; Nithitanakul, M.; Supaphol, P. Ultrafine Electrospun Polyamide-6 Fibers: Effect of Solution Conditions on Morphology and Average Fiber Diameter. *Macromol. Chem. Phys.* **2004**, *205*, 2327–2338. [CrossRef]
44. Casper, C.L.; Stephens, J.S.; Tassi, N.G.; Chase, D.B.; Rabolt, J.F. Controlling Surface Morphology of Electrospun Polystyrene Fibers: Effect of Humidity and Molecular Weight in the Electrospinning Process. *Macromolecules* **2004**, *37*, 573–578. [CrossRef]
45. Kugarajah, V.; Ojha, A.K.; Ranjan, S.; Dasgupta, N.; Ganesapillai, M.; Dharmalingam, S.; Elmoll, A.; Hosseini, S.A.; Muthulakshmi, L.; Vijayakumar, S.; et al. Future applications of electrospun nanofibers in pressure driven water treatment: A brief review and research update. *J. Environ. Chem. Eng.* **2021**, *9*, 105107. [CrossRef]
46. Saleem, H.; Trabzon, L.; Kilic, A.; Zaidi, S.J. Recent advances in nanofibrous membranes: Production and applications in water treatment and desalination. *Desalination* **2020**, *478*, 114178. [CrossRef]
47. Ravi, J.; Othman, M.H.D.; Matsuura, T.; Bilad, M.R.; El-Badawy, T.; Aziz, F.; Ismail, A.; Rahman, M.A.; Jaafar, J. Polymeric membranes for desalination using membrane distillation: A review. *Desalination* **2020**, *490*, 114530. [CrossRef]
48. Li, C.; Li, X.; Du, X.; Zhang, Y.; Wang, W.; Tong, T.; Kota, A.K.; Lee, J. Elucidating the Trade-off between Membrane Wetting Resistance and Water Vapor Flux in Membrane Distillation. *Environ. Sci. Technol.* **2020**, *54*, 10333–10341. [CrossRef]
49. Sadeghzadeh, A.; Bazgir, S.; Shirazi, M.M.A. Fabrication and characterization of a novel hydrophobic polystyrene membrane using electroblowing technique for desalination by direct contact membrane distillation. *Sep. Purif. Technol.* **2020**, *239*, 116498. [CrossRef]
50. Ricceri, F.; Giagnorio, M.; Farinelli, G.; Blandini, G.; Minella, M.; Vione, D.; Tiraferri, A. Desalination of Produced Water by Membrane Distillation: Effect of the Feed Components and of a Pre-treatment by Fenton Oxidation. *Sci. Rep.* **2019**, *9*, 1–12. [CrossRef]
51. Gontarek-Castro, E.; Castro-Muñoz, R.; Lieder, M. New insights of nanomaterials usage toward superhydrophobic membranes for water desalination via membrane distillation: A review. *Crit. Rev. Environ. Sci. Technol.* **2021**, 1–46. [CrossRef]
52. Li, K.; Hou, D.; Fu, C.; Wang, K.; Wang, J. Fabrication of PVDF nanofibrous hydrophobic composite membranes reinforced with fabric substrates via electrospinning for membrane distillation desalination. *J. Environ. Sci.* **2019**, *75*, 277–288. [CrossRef]
53. An, A.K.; Lee, E.-J.; Guo, J.; Jeong, S.; Lee, J.-G.; Ghaffour, N. Enhanced vapor transport in membrane distillation via functionalized carbon nanotubes anchored into electrospun nanofibres. *Sci. Rep.* **2017**, *7*, 1–11. [CrossRef]
54. Fouladivanda, M.; Karimi-Sabet, J.; Abbasi, F.; Moosavian, M.A. Step-by-step improvement of mixed-matrix nanofiber membrane with functionalized graphene oxide for desalination via air-gap membrane distillation. *Sep. Purif. Technol.* **2021**, *256*, 117809. [CrossRef]
55. Lee, D.; Woo, Y.C.; Park, K.H.; Phuntsho, S.; Tijing, L.D.; Yao, M.; Shim, W.-G.; Shon, H.K. Polyvinylidene fluoride phase design by two-dimensional boron nitride enables enhanced performance and stability for seawater desalination. *J. Membr. Sci.* **2020**, *598*, 117669. [CrossRef]
56. Tijing, L.D.; Woo, Y.C.; Shim, W.-G.; He, T.; Choi, J.-S.; Kim, S.-H.; Shon, H.K. Superhydrophobic nanofiber membrane containing carbon nanotubes for high-performance direct contact membrane distillation. *J. Membr. Sci.* **2016**, *502*, 158–170. [CrossRef]
57. Woo, Y.C.; Tijing, L.; Shim, W.-G.; Choi, J.-S.; Kim, S.-H.; He, T.; Drioli, E.; Shon, H.K. Water desalination using graphene-enhanced electrospun nanofiber membrane via air gap membrane distillation. *J. Membr. Sci.* **2016**, *520*, 99–110. [CrossRef]

58. Hou, D.; Ding, C.; Fu, C.; Wang, D.; Zhao, C.; Wang, J. Electrospun nanofibrous omniphobic membrane for anti-surfactant-wetting membrane distillation desalination. *Desalination* **2019**, *468*, 114068. [CrossRef]
59. Woo, Y.C.; Tijing, L.D.; Park, M.J.; Yao, M.; Choi, J.-S.; Lee, S.; Kim, S.-H.; An, A.K.; Shon, H.K. Electrospun dual-layer nonwoven membrane for desalination by air gap membrane distillation. *Desalination* **2017**, *403*, 187–198. [CrossRef]
60. Zhao, L.; Wu, C.; Lu, X.; Ng, D.; Truong, Y.B.; Xie, Z. Activated carbon enhanced hydrophobic/hydrophilic dual-layer nanofiber composite membranes for high-performance direct contact membrane distillation. *Desalination* **2018**, *446*, 59–69. [CrossRef]
61. Khayet, M.; García-Payo, C.; Matsuura, T. Superhydrophobic nanofibers electrospun by surface segregating fluorinated amphiphilic additive for membrane distillation. *J. Membr. Sci.* **2019**, *588*, 117215. [CrossRef]
62. Dong, Z.; Ma, X.-H.; Xu, Z.-L.; You, W.-T.; Li, F.-B. Superhydrophobic PVDF–PTFE electrospun nanofibrous membranes for desalination by vacuum membrane distillation. *Desalination* **2014**, *347*, 175–183. [CrossRef]
63. Yan, K.-K.; Jiao, L.; Lin, S.; Ji, X.; Lu, Y.; Zhang, L. Superhydrophobic electrospun nanofiber membrane coated by carbon nanotubes network for membrane distillation. *Desalination* **2018**, *437*, 26–33. [CrossRef]
64. Li, X.; García-Payo, C.; Khayet, M.; Wang, M.; Wang, X. Superhydrophobic polysulfone/polydimethylsiloxane electrospun nanofibrous membranes for water desalination by direct contact membrane distillation. *J. Membr. Sci.* **2017**, *542*, 308–319. [CrossRef]
65. Li, H.; Shi, W.; Zeng, X.; Huang, S.; Zhang, H.; Qin, X. Improved desalination properties of hydrophobic GO-incorporated PVDF electrospun nanofibrous composites for vacuum membrane distillation. *Sep. Purif. Technol.* **2020**, *230*, 115889. [CrossRef]
66. Wang, X.; Ma, H.; Chu, B.; Hsiao, B.S. Thin-film nanofibrous composite reverse osmosis membranes for desalination. *Desalination* **2017**, *420*, 91–98. [CrossRef]
67. Cruz-Silva, R.; Izu, K.; Maeda, J.; Saito, S.; Morelos-Gomez, A.; Aguilar, C.; Takizawa, Y.; Yamanaka, A.; Tejiima, S.; Fujisawa, K.; et al. Nanocomposite desalination membranes made of aromatic polyamide with cellulose nanofibers: Synthesis, performance, and water diffusion study. *Nanoscale* **2020**, *12*, 19628–19637. [CrossRef]
68. Liu, S.; Low, Z.-X.; Hegab, H.M.; Xie, Z.; Ou, R.; Yang, G.; Simon, G.P.; Zhang, X.; Zhang, L.; Wang, H. Enhancement of desalination performance of thin-film nanocomposite membrane by cellulose nanofibers. *J. Membr. Sci.* **2019**, *592*, 117363. [CrossRef]
69. Kim, S.; Heath, D.E.; Kentish, S.E. Composite Membranes with Nanofibrous Cross-Hatched Supports for Reverse Osmosis Desalination. *ACS Appl. Mater. Interfaces* **2020**, *12*, 44720–44730. [CrossRef]
70. Shibuya, M.; Park, M.J.; Lim, S.; Phuntsho, S.; Matsuyama, H.; Shon, H.K. Novel CA/PVDF nanofiber supports strategically designed via coaxial electrospinning for high performance thin-film composite forward osmosis membranes for desalination. *Desalination* **2018**, *445*, 63–74. [CrossRef]
71. Al-Furaiji, M.; Kadhom, M.; Kalash, K.; Waisi, B.; Albayati, N. Preparation of TFC Membranes Sup-ported with Elelctrospun Nanofibers for Desalination by Forward Osmosis. *Drink. Water Eng. Sci. Discuss.* **2020**, *2020*, 1–17. [CrossRef]
72. Obaid, M.; Ghouri, Z.K.; Fadali, O.A.; Khalil, K.A.; Almajid, A.A.; Barakat, N.A.M. Amorphous SiO2 NP-Incorporated Poly(vinylidene fluoride) Electrospun Nanofiber Membrane for High Flux Forward Osmosis Desalination. *ACS Appl. Mater. Interfaces* **2016**, *8*, 4561–4574. [CrossRef]
73. Jain, H.; Garg, M.C. Fabrication of polymeric nanocomposite forward osmosis membranes for water desalination—A review. *Environ. Technol. Innov.* **2021**, *23*, 101561. [CrossRef]
74. Li, Y.; Wong, E.; Mai, Z.; Van der Bruggen, B. Fabrication of composite polyamide/Kevlar aramid nanofiber nanofiltration membranes with high permselectivity in water desalination. *J. Membr. Sci.* **2019**, *592*, 117396. [CrossRef]
75. Liua, Y.; Gaoa, X.; Zhangb, L.; Shenc, X.; Dua, X.; Doua, X.; Yuana, X. Mn2O3 nanoflower decorated electrospun carbon nanofibers for efficient hybrid capacitive deionization. *Desalination* **2020**, *494*, 114665. [CrossRef]
76. Sokolowski, K.; Blazewicz, S.; Nocun, M.; Fraczek-Szczypta, A. Carbon micro- and nanofibrous materials with high adsorption capacity for water desalination. *Desalination* **2021**, *503*, 114936. [CrossRef]
77. Fan, Y.; Chen, S.; Zhao, H.; Liu, Y. Distillation membrane constructed by TiO_2 nanofiber followed by fluorination for excellent water desalination performance. *Desalination* **2017**, *405*, 51–58. [CrossRef]
78. Subramanian, S.; Seeram, R. New directions in nanofiltration applications—Are nanofibers the right materials as membranes in desalination? *Desalination* **2013**, *308*, 198–208. [CrossRef]
79. Feng, C.; Khulbe, K.; Matsuura, T.; Tabe, S.; Ismail, A. Preparation and characterization of electro-spun nanofiber membranes and their possible applications in water treatment. *Sep. Purif. Technol.* **2013**, *102*, 118–135. [CrossRef]
80. Cui, J.; Li, F.; Wang, Y.; Zhang, Q.; Ma, W.; Huang, C. Electrospun nanofiber membranes for wastewater treatment applications. *Sep. Purif. Technol.* **2020**, *250*, 117116. [CrossRef]
81. Woo, Y.C.; Yao, M.; Shim, W.-G.; Kim, Y.; Tijing, L.D.; Jung, B.; Kim, S.-H.; Shon, H.K. Co-axially electrospun superhydrophobic nanofiber membranes with 3D-hierarchically structured surface for desalination by long-term membrane distillation. *J. Membr. Sci.* **2021**, *623*, 119028. [CrossRef]
82. Yang, F.; Efome, J.E.; Rana, D.; Matsuura, T.; Lan, C. Metal–Organic Frameworks Supported on Nanofiber for Desalination by Direct Contact Membrane Distillation. *ACS Appl. Mater. Interfaces* **2018**, *10*, 11251–11260. [CrossRef]
83. Nuraje, N.; Khan, W.S.; Lei, Y.; Ceylan, M.; Asmatulu, R. Superhydrophobic electrospun nanofibers. *J. Mater. Chem. A* **2013**, *1*, 1929–1946. [CrossRef]
84. Niknejad, A.S.; Bazgir, S.; Kargari, A. Desalination by direct contact membrane distillation using a superhydrophobic nanofibrous poly (methyl methacrylate) membrane. *Desalination* **2021**, *511*, 115108. [CrossRef]

85. Li, Z.; Cheng, B.; Ju, J.; Kang, W.; Liu, Y. Development of a novel multi-scale structured superhydrophobic nanofiber membrane with enhanced thermal efficiency and high flux for membrane distillation. *Desalination* **2021**, *501*, 114834. [CrossRef]
86. Nthunya, L.N.; Gutierrez, L.; Lapeire, L.; Verbeken, K.; Zaouri, N.; Nxumalo, E.N.; Mamba, B.; Verliefde, A.R.; Mhlanga, S. Fouling-resistant PVDF nanofibre membranes for the desalination of brackish water in membrane distillation. *Sep. Purif. Technol.* **2019**, *228*, 115793. [CrossRef]
87. Li, Z.; Liu, Y.; Yan, J.; Wang, K.; Xie, B.; Hu, Y.; Kang, W.; Cheng, B. Electrospun polyvinylidene fluoride/fluorinated acrylate copolymer tree-like nanofiber membrane with high flux and salt rejection ratio for direct contact membrane distillation. *Desalination* **2019**, *466*, 68–76. [CrossRef]
88. Ray, S.S.; Chen, S.-S.; Nguyen, N.C.; Hsu, H.-T.; Nguyen, H.T.; Chang, C.-T. Poly(vinyl alcohol) incorporated with surfactant based electrospun nanofibrous layer onto polypropylene mat for improved desalination by using membrane distillation. *Desalination* **2017**, *414*, 18–27. [CrossRef]
89. Hou, D.; Ding, C.; Li, K.; Lin, D.; Wang, D.; Wang, J. A novel dual-layer composite membrane with underwater-superoleophobic/hydrophobic asymmetric wettability for robust oil-fouling resistance in membrane distillation desalination. *Desalination* **2018**, *428*, 240–249. [CrossRef]
90. Hammami, M.; Croissant, J.; Francis, L.; Alsaiari, S.; Anjum, D.H.; Ghaffour, N.; Khashab, N.M. Engineering Hydrophobic Organosilica Nanoparticle-Doped Nanofibers for Enhanced and Fouling Resistant Membrane Distillation. *ACS Appl. Mater. Interfaces* **2017**, *9*, 1737–1745. [CrossRef]
91. Woo, Y.C.; Chen, Y.; Tijing, L.; Phuntsho, S.; He, T.; Choi, J.-S.; Kim, S.-H.; Shon, H.K. CF4 plasma-modified omniphobic electrospun nanofiber membrane for produced water brine treatment by membrane distillation. *J. Membr. Sci.* **2017**, *529*, 234–242. [CrossRef]
92. Niknejad, A.S.; Bazgir, S.; Sadeghzadeh, A.; Shirazi, M.M.A. Styrene-acrylonitrile (SAN) nanofibrous membranes with unique properties for desalination by direct contact membrane distillation (DCMD) process. *Desalination* **2020**, *488*, 114502. [CrossRef]
93. Al-Furaiji, M.; Kadhom, M.; Kalash, K.; Waisi, B.; Albayati, N. Preparation of thin-film composite membranes supported with electrospun nanofibers for desalination by forward osmosis. *Drink. Water Eng. Sci.* **2020**, *13*, 51–57. [CrossRef]
94. Park, S.H.; Kim, J.H.; Moon, S.J.; Drioli, E.; Lee, Y.M. Enhanced, hydrophobic, fluorine-containing, thermally rearranged (TR) nanofiber membranes for desalination via membrane distillation. *J. Membr. Sci.* **2018**, *550*, 545–553. [CrossRef]
95. Chiam, C.K.; Sarbatly, R.; Widyaparamitha, S. Investigating the potential of meltblown polypropylene nanofiber membrane for desalination by membrane distillation. *IOP Conf. Ser. Mater. Sci. Eng.* **2019**, *606*, 012012. [CrossRef]
96. Rosalam, S.; Chiam, C.K.; Widyaparamitha, S.; Chang, Y.W.; Lee, C.A. Water desalination by air-gap membrane distillation using meltblown polypropylene nanofiber membrane. *IOP Conf. Ser. Earth Environ. Sci.* **2016**, *36*, 12032. [CrossRef]
97. Yang, J.; Hou, B.; Wang, J.; Tian, B.; Bi, J.; Wang, N.; Li, X.; Huang, X. Nanomaterials for the Removal of Heavy Metals from Wastewater. *Nanomaterials* **2019**, *9*, 424. [CrossRef] [PubMed]
98. Ortiz, J.E.; Chabot, B. Electrospun nanofibers for the removal of heavy metals from aqueous solutions. *Mitacs Glob. Intership Rep. Monterrey Mex. Monterrey Inst. Technol. High. Educ.* **2016**, 1–22. [CrossRef]
99. Ligneris, E.D.; Dumée, L.F.; Kong, L. Nanofibers for heavy metal ion adsorption: Correlating surface properties to adsorption performance, and strategies for ion selectivity and recovery. *Environ. Nanotechnol. Monit. Manag.* **2020**, *13*, 100297. [CrossRef]
100. Li, S.; Yue, X.; Jing, Y.; Bai, S.; Dai, Z. Fabrication of zonal thiol-functionalized silica nanofibers for removal of heavy metal ions from wastewater. *Colloids Surf. A Physicochem. Eng. Asp.* **2011**, *380*, 229–233. [CrossRef]
101. Zhu, F.; Zheng, Y.-M.; Zhang, B.-G.; Dai, Y.-R. A critical review on the electrospun nanofibrous membranes for the adsorption of heavy metals in water treatment. *J. Hazard. Mater.* **2021**, *401*, 123608. [CrossRef]
102. Vo, T.S.; Hossain, M.M.; Jeong, H.M.; Kim, K. Heavy metal removal applications using adsorptive membranes. *Nano Converg.* **2020**, *7*, 36. [CrossRef]
103. Baskar, D.; Selvam, A.K.; Ganesan, M.; Nallathambi, G. Mechanism of Nanofibres on Removal of Wa-Ter Pollutants—A Review. *Indian J. Chem. Technol.* **2018**, *25*, 451–458.
104. Wang, J.; Luo, C.; Qi, G.; Pan, K.; Cao, B. Mechanism study of selective heavy metal ion removal with polypyrrole-functionalized polyacrylonitrile nanofiber mats. *Appl. Surf. Sci.* **2014**, *316*, 245–250. [CrossRef]
105. Almasian, A.; Najafi, F.; Maleknia, L.; Giahi, M. Mesoporous MgO/PPG hybrid nanofibers: Synthesis, optimization, characterization and heavy metal removal property. *New J. Chem.* **2017**, *42*, 2013–2029. [CrossRef]
106. Fatma, Y. A review on advanced nanofiber technology for membrane distillation. *J. Eng. Fibers Fabr.* **2019**, *14*, 1–12. [CrossRef]
107. Deng, S.; Liu, X.; Liao, J.; Lin, H.; Liu, F. PEI modified multiwalled carbon nanotube as a novel additive in PAN nanofiber membrane for enhanced removal of heavy metal ions. *Chem. Eng. J.* **2019**, *375*, 122086. [CrossRef]
108. Sankararamakrishnan, N.; Singh, R.; Srivastava, I. Performance of novel MgS doped cellulose nanofibres for Cd(II) removal from industrial effluent—Mechanism and optimization. *Sci. Rep.* **2019**, *9*, 1–8. [CrossRef]
109. Ebrahimi, F.; Sadeghizadeh, A.; Neysan, F.; Heydari, M. Fabrication of nanofibers using sodium alginate and Poly(Vinyl alcohol) for the removal of Cd2+ ions from aqueous solutions: Adsorption mechanism, kinetics and thermodynamics. *Heliyon* **2019**, *5*, e02941. [CrossRef]
110. Martín, D.M.; Faccini, M.; García, M.; Amantia, D. Highly efficient removal of heavy metal ions from polluted water using ion-selective polyacrylonitrile nanofibers. *J. Environ. Chem. Eng.* **2018**, *6*, 236–245. [CrossRef]

111. Jiang, M.; Han, T.; Wang, J.; Shao, L.; Qi, C.; Zhang, X.M.; Liu, C.; Liu, X. Removal of heavy metal chromium using cross-linked chitosan composite nanofiber mats. *Int. J. Biol. Macromol.* **2018**, *120*, 213–221. [CrossRef]
112. Xu, D.; Zhu, K.; Zheng, X.; Xiao, R. Poly(ethylene-co-vinyl alcohol) Functional Nanofiber Membranes for the Removal of Cr(VI) from Water. *Ind. Eng. Chem. Res.* **2015**, *54*, 6836–6844. [CrossRef]
113. Abbasizadeh, S.; Keshtkar, A.R.; Mousavian, M.A. Preparation of a novel electrospun polyvinyl alco-hol/titanium oxide nanofiber adsorbent modified with mercapto groups for uranium(VI) and thorium(IV) re-moval from aqueous solution. *Chem. Eng. J.* **2013**, *220*, 161–171. [CrossRef]
114. Alipour, D.; Keshtkar, A.R.; Moosavian, M.A. Adsorption of thorium(IV) from simulated radioactive solutions using a novel electrospun PVA/TiO2/ZnO nanofiber adsorbent functionalized with mercapto groups: Study in single and multi-component systems. *Appl. Surf. Sci.* **2016**, *366*, 19–29. [CrossRef]
115. Ahmad, M.; Wang, J.; Xu, J.; Zhang, Q.; Zhang, B. Magnetic tubular carbon nanofibers as efficient Cu(II) ion adsorbent from wastewater. *J. Clean. Prod.* **2020**, *252*, 119825. [CrossRef]
116. Yang, D.; Zheng, Z.; Liu, H.; Zhu, H.Y.; Ke, X.; Xu, Y.; Wu, D.; Sun, Y. Layered Titanate Nanofibers as Efficient Adsorbents for Removal of Toxic Radioactive and Heavy Metal Ions from Water. *J. Phys. Chem. C* **2008**, *112*, 16275–16280. [CrossRef]
117. Nawaz, T.; Sengupta, S. Contaminants of Emerging Concern: Occurrence, Fate, and Remediation. *Adv. Water Purif. Tech.* **2019**, 67–114. [CrossRef]
118. Deblonde, T.; Cossu-Leguille, C.; Hartemann, P. Emerging pollutants in wastewater: A review of the literature. *Int. J. Hyg. Environ. Health* **2011**, *214*, 442–448. [CrossRef]
119. Glassmeyer, S.T.; Furlong, E.T.; Kolpin, D.W.; Batt, A.L.; Benson, R.; Boone, J.S.; Wilson, V.S. Na-tionwide reconnaissance of contaminants of emerging concern in source and treated drinking waters of the United States. *Sci. Total. Environ.* **2017**, *581*, 909–922. [CrossRef]
120. Camiré, A.; Espinasse, J.; Chabot, B.; Lajeunesse, A. Development of electrospun lignin nanofibers for the adsorption of pharmaceutical contaminants in wastewater. *Environ. Sci. Pollut. Res.* **2020**, *27*, 3560–3573. [CrossRef]
121. Peter, K.; Vargo, J.D.; Rupasinghe, T.P.; De Jesus, A.; Tivanski, A.V.; Sander, E.A.; Myung, N.V.; Cwiertny, D.M. Synthesis, Optimization, and Performance Demonstration of Electrospun Carbon Nanofiber–Carbon Nanotube Composite Sorbents for Point-of-Use Water Treatment. *ACS Appl. Mater. Interfaces* **2016**, *8*, 11431–11440. [CrossRef]
122. Chabalala, M.B.; Al-Abri, M.Z.; Mamba, B.B.; Nxumalo, E.N. Mechanistic aspects for the enhanced adsorption of bromophenol blue and atrazine over cyclodextrin modified polyacrylonitrile nanofiber mem-branes. *Chem. Eng. Res. Des.* **2021**, *169*, 19–32. [CrossRef]
123. Lv, Y.; Ma, J.; Liu, K.; Jiang, Y.; Yang, G.; Liu, Y.; Chen, L. Rapid elimination of trace bisphenol pol-lutants with porous β-cyclodextrin modified cellulose nanofibrous membrane in water: Adsorption behavior and mechanism. *J. Hazard. Mater.* **2021**, *403*, 123666. [CrossRef] [PubMed]
124. Khalil, A.M.; Schäfer, A.I. Cross-linked β-cyclodextrin nanofiber composite membrane for steroid hormone micropollutant removal from water. *J. Membr. Sci.* **2021**, *618*, 118228. [CrossRef]
125. Khalil, A.M.; Hashem, T.; Gopalakrishnan, A.; Schäfer, A.I. Cyclodextrin Composite Nanofiber Membrane: Impact of the Crosslinker Type on Steroid Hormone Micropollutant Removal from Water. *ACS Appl. Polym. Mater.* **2021**, *3*, 2646–2656. [CrossRef]
126. Nor, N.A.M.; Jaafar, J.; Ismail, A.F.; Mohamed, M.A.; Rahman, M.A.; Othman, M.H.D.; Yusof, N. Preparation and performance of PVDF-based nanocomposite membrane consisting of TiO2 nanofibers for or-ganic pollutant decomposition in wastewater under UV irradiation. *Desalination* **2016**, *391*, 89–97. [CrossRef]
127. Gadisa, B.T.; Kassahun, S.K.; Appiah-Ntiamoah, R.; Kim, H. Tuning the charge carrier density and exciton pair separation in electrospun 1D ZnO-C composite nanofibers and its effect on photodegradation of emerging contaminants. *J. Colloid Interface Sci.* **2020**, *570*, 251–263. [CrossRef]
128. Ramasundaram, S.; Yoo, H.N.; Song, K.G.; Lee, J.; Choi, K.J.; Hong, S.W. Titanium dioxide nano-fibers integrated stainless steel filter for photocatalytic degradation of pharmaceutical compounds. *J. Hazard. Mater.* **2013**, *258*, 124–132. [CrossRef]
129. Chen, S.; Li, M.; Zhang, M.; Wang, C.; Luo, R.; Yan, X.; Zhang, H.; Qi, J.; Sun, X.; Li, J. Metal organic framework derived one-dimensional porous Fe/N-doped carbon nanofibers with enhanced catalytic performance. *J. Hazard. Mater.* **2021**, *416*, 126101. [CrossRef]
130. Greenstein, K.E.; Nagorzanski, M.R.; Kelsay, B.; Verdugo, E.M.; Myung, N.V.; Parkin, G.F.; Cwiertny, D.M. Carbon–titanium dioxide (C/TiO_2) nanofiber composites for chemical oxidation of emerging organic contaminants in reactive filtration applications. *Environ. Sci. Nano* **2021**, *8*, 711–722. [CrossRef]
131. Kim, J.-C.; Oh, S.-I.; Kang, W.; Yoo, H.-Y.; Lee, J.; Kim, D.-W. Superior anodic oxidation in tailored Sb-doped SnO_2/RuO_2 composite nanofibers for electrochemical water treatment. *J. Catal.* **2019**, *374*, 118–126. [CrossRef]
132. Xie, W.; Shi, Y.; Wang, Y.; Zheng, Y.; Liu, H.; Hu, Q.; Guo, Z. Electrospun iron/cobalt alloy nanopar-ticles on carbon nanofibers towards exhaustive electrocatalytic degradation of tetracycline in wastewater. *Chem. Eng. J.* **2021**, *405*, 126585. [CrossRef]
133. Yang, G.C.; Yen, C.H. The use of different materials to form the intermediate layers of tubular car-bon nanofibers/carbon/alumina composite membranes for removing pharmaceuticals from aqueous solu-tions. *J. Membr. Sci.* **2013**, *425*, 121–130. [CrossRef]